We are IntechOpen,
the world's leading publisher of
Open Access books
Built by scientists, for scientists

6,900
Open access books available

186,000
International authors and editors

200M
Downloads

Our authors are among the

154
Countries delivered to

TOP 1%
most cited scientists

12.2%
Contributors from top 500 universities

CLARIVATE ANALYTICS
BOOK CITATION INDEX
INDEXED

WEB OF SCIENCE™

Selection of our books indexed in the Book Citation Index
in Web of Science™ Core Collection (BKCI)

Interested in publishing with us?
Contact book.department@intechopen.com

Numbers displayed above are based on latest data collected.
For more information visit www.intechopen.com

Wavelet Signatures and Diagnostics for the Assessment of ICU Agitation-Sedation Protocols

In Kang, Irene Hudson, Andrew Rudge and J. Geoffrey Chase
[1]*Department of Mathematics and Statistics, University of Canterbury, Christchurch,*
[2]*School of Mathematical and Physical Sciences, University of Newcastle, NSW,*
[3]*Faculty of Health, Engineering and Science Victoria University, Melbourne,*
[4]*Department of Mechanical Engineering, University of Canterbury Christchurch,*
[1,4]*New Zealand*
[2,3]*Australia*

1. Introduction

The use of quantitative modelling to enhance understanding of the agitation-sedation (A-S) system and the provision of an A-S simulation platform are key tools in this area of patient critical care. A suite of wavelet techniques and metrics based on the discrete wavelet transform (DWT) are developed in this chapter which are shown to successfully establish the validity of deterministic agitation-sedation (A-S) models against empirical (recorded) dynamic A-S infusion profiles. The DWT approach is shown to provide robust performance metrics of A-S control and also yield excellent visual assessment tools. This approach is generalisable to any study which investigates the similarity or closeness of bivariate time series of, say, a large number of units (patients, households etc) and of disparate lengths and of possibly extremely long length. This work demonstrates the value of the DWT for assessing ICU agitation-sedation deterministic models, and suggests new wavelet based diagnostics by which to assess the A-S models.

Typically agitation-sedation cycling in critically ill patients involves oscillations between states of agitation and over-sedation, which is detrimental to patient health, and increases hospital length of stay (Rudge et al., 2006a; 2006b; Chase et al., 2004; Rudge et al 2005). Agitation management via effective sedation management is an important and fundamental activity in the intensive care unit (ICU), where in the hospitalized adult agitation is defined as excessive verbal behaviour that interferes with patient care, and the patient's medical therapies (Chase et al., 2004).   The main goal of sedation is to control agitation, while also preventing over-sedation and over-use of drugs. In clinical practice, however, a lack of understanding of the underlying dynamics of A-S, combined with a lack of subjective assessment tools, makes effective and consistent clinical agitation management difficult (Chase et al., 2004; Rudge et al., 2005, 2006b). Early agitation management methods traditionally relied on subjective agitation assessment, and sedation assessment scales, combined with medical staff experience and intuition, to deliver appropriate sedation; and an appropriate sedation input response, from recorded at bedside agitation scales (Fraser &

Riker, 2001b; Jaarsma et al., 2001; Ramsay et al., 1974; Ricker et al., 1999; Sessler et al., 2002). The clinical staff at the bedside, usually nurses, then select an appropriate infusion rate based upon their evaluation of these scales, experience, and intuition (Kress et al., 2002). This approach usually leads to the administration of largely continuous infusions which lack a bolus-focused approach, and commonly result in either over sedation, or insufficient sedation (Rudge et al., 2006b). Several recent studies have emphasised the cost and healthcare advantages of drug delivery protocols based on assessment scales of agitation and sedation. A minimal differential equation (DE) model to predict or simulate the patients' agitation-sedation status over time (range [3,001-25,261] time points in minutes) was developed and validated statistically for the first time by Chase et al. (2004). This process is depicted in Figure 3 (see Chase et al., 2004). The goal of the research was to create a physiologically representative pharmacodynamic model that captured the fundamental dynamics of the A-S system. The resulting model can serve as a platform to develop and test semi-automated sedation management controllers that offer the potential of improved agitation management and thus, the clinically relevant outcomes of reduced length of stay in the ICU and reduced health care costs as a result. A-S models were later developed by Rudge et al. (2005, 2006a, 2006b). All these models used either kernel regression, tracking indices, kernel density estimation, a probability band or time within a band as metrics of similarity or closeness of the patient's simulated and recorded A-S profiles. Lee et al. (2005) also developed a nonparametric regression approach with an Epanechnikov kernel (Wand & Jones 1995) to assess the validity of the deterministic A-S models.

The work in this chapter develops novel wavelet signatures and wavelet based statistics and threshold criterion (to assess closeness between pairs of time series). These are applied to the recorded and the simulated infusion rates obtained from the DE models of Chase et al. (2004) to test for commonality across patients, in terms of wavelet correlations. A major aim of this study is to test the feasibility of wavelet statistics to help distinguish between patients whose simulated profiles were "close" to their mean profile a majority of the time profile versus those for whom this was not the case - so-called good versus poor trackers. This research builds on initial work by Kang et al. (2005), which was a preliminary study to assess wavelet signatures for modelling ICU A-S profiles to evaluate "closeness" or "discrimination" of simulated versus actual A-S profiles with respect to wavelet scales. Another earlier application of some of our methods was the study by Kang et al. (2004) on historical, flowering records of 4 Eucalypt species, where it was established that wavelets add credibility to the use of phenological records to detect climate change (see also Hudson, 2010, Hudson 2011, Hudson et al., 2010c and Hudson et al., 2005). This early phenological study was recently expanded from 4 to 8 Eucalypt species by Hudson et al. (2011a, 2011b) (see also Hudson et al., 2010a, 2010b and Hudson & Keatley, 2010).

2. Brief review of wavelets and associated mathematics

Section 2 gives a brief introduction of the basic ideas concerning wavelets. A wave is usually defined as an oscillating function that is localized in both time and frequency. A wavelet is a "small wave", which has its energy concentrated in time to give a tool for the analysis of transient, nonstationary, or time-varying phenomena (Goupillaud et al., 1984; Morlet, 1983). Wavelets have the ability to allow simultaneous time and frequency analysis via a flexible mathematical foundation. Wavelets are well suited to the analysis of transient signals in particular. The localizing property of wavelets allows a wavelet expansion of a transient

component on an orthogonal basis to be modelled using a small number of wavelet coefficients using a low pass filter (Barber et al., 2002). This allows application to a wide range of fields, such as signal processing, data compression, and image analysis (Mallat, 1998; Meyer, 2003; Kumar, 1993, 1994; Donoho, 1995; Chang et al., 2000a, 2000b). The wavelet decomposition of functions is analogous to Fourier decomposition methods (Ogden, 1997; Abramovich & Benjamini, 1995). The wavelet representation is presented first in terms of its simplest paradigm, the Haar wavelet (Haar, 1910). The Haar wavelet is used here to describe the concepts of multiresolution analysis (MRA). For more details about wavelets see, for example, Daubeches (1992), Chui (1992), Donoho & Johnstone (1994), Ogden (1997), Vidakovic (1999), Percival & Walden (2000), and Gencay et al. (2001).

2.1 The Discrete Wavelet Transform (DWT)

Wavelets may be formed from the mother wavelet function $\psi(t)$ via dyadic dilation and integer translation by the following,

$$\psi_{j,k}(t) = 2^{j/2} \psi(2^j t - k) \quad j, k \in Z, \tag{1}$$

where $\mathbb{Z}$ is the set of all integers and the factor $2^{j/2}$ maintains a constant norm independent of scale j. The entire set of wavelets $\psi_{j,k}(t)$ forms an orthonormal basis (Daubeches, 1992). The wavelet functions $\psi_{j,k}$ are ordered according to their dilation index j and translation index k. Higher j corresponds to lower frequency wavelets, and higher k corresponds to a rightward shift. The wavelet transform is usually considered to be a continuous wavelet transform (CWT) (Vidakovic, 1999; Percival & Walden, 2000; Gencay et al., 2001) since it is applied to a function $f(\cdot)$ defined over the entire real axis. However, we only have a finite number N of sampled values, as is usually the case for real data applications. This approach leads to the discrete wavelet transform (DWT). To some degree of approximation, we can regard the DWT as being formed by taking slices through a corresponding CWT (McCoy et al., 1995). Any wavelet in $L^2(R)$ then can then be written as a set of expansion functions,

$$f(t) = \sum_{j,k} a_{j,k} 2^{j/2} \psi\left(2^j t - k\right) \tag{2}$$

where the two-dimensional set of coefficients $a_{j,k}$ is called the discrete wavelet transform of $f(t)$. A more specific form indicating how the $a_{j,k}$'s are calculated, can be written using inner products (Swelden, 1996) as follows,

$$f(t) = \sum_{j,k} \left\langle f(t), \psi_{j,k}(t) \right\rangle \psi_{j,k}(t). \tag{3}$$

Let X_t be a dyadic length column vector containing a sequence $X_1, X_2, \cdots, X_N$ of $N = 2^J$ observations of a real-valued time series. The length N vector of discrete wavelet coefficients W is obtained via $W = \mathcal{W}X$, where $\mathcal{W}$ is an $N \times N$ orthonormal matrix defining the DWT. The vector of wavelet coefficients may be organised into $J + 1$ vectors,

$$W = \left[W_1, W_2, \cdots, W_J, V_J \right]^T \tag{4}$$

where W_j is a length $N/2^j$ vector of wavelet coefficients associated with changes on a scale of length $\lambda_j = 2^{j-1}$ and V_J is a length $N/2^J$ vector scaling coefficients associated with averages on a scale of length $2^J = 2\lambda_J$. Wavelet coefficients thus tell us about variations in adjacent averages (Percival & Walden, 2000).

The structure of the $N \times N$ dimensional matrix $\mathcal{W}$ is visualised through the submatrices $\mathcal{W}_1, \ldots, \mathcal{W}_J$ and $\mathcal{V}_J$ (scaling coefficient matrix) via

$$\mathcal{W} = \left[\mathcal{W}_1, \mathcal{W}_2, \ldots, \mathcal{W}_J, \mathcal{V}_J \right]^T . \tag{5}$$

Let us now consider implementation of the DWT by using a pyramid algorithm (PA) (Mallat, 1989). Let $h = (h_0, \ldots, h_{L-1})$ be the vector of wavelet (high-pass) filter coefficients and $g = (g_0, \ldots, g_{L-1})$ be the vector of scaling (low-pass) filter coefficients (Daubechies, 1992). Graphical representation of the DWT as applied to a dyadic length vector X_t is given by Figure 1 and Figure 2. These depict the analysis of X_t into $\mathcal{W}_1$, $\mathcal{W}_2$ and $\mathcal{V}_2$ using the pyramid algorithm (PA). The synthesis of X_t from $\mathcal{W}_1$, $\mathcal{W}_2$ and $\mathcal{V}_2$ use the inverse of the PA (Figure 2).
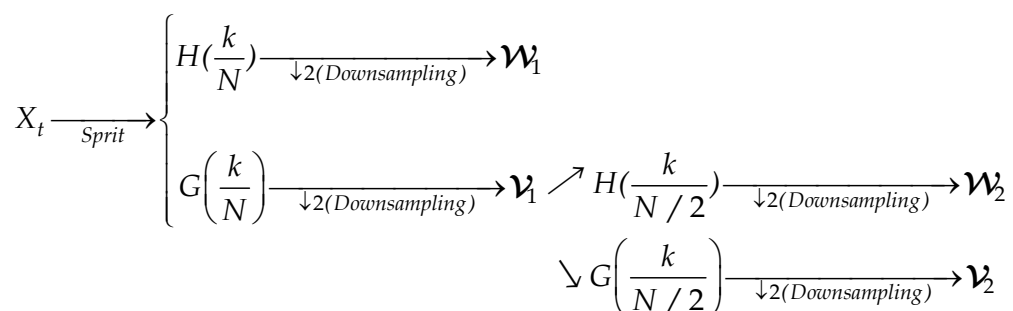

Fig. 1. Flow diagram illustrating the decomposition of X_t into first and second level wavelet coefficients $\mathcal{W}_{1,t}$ and $\mathcal{W}_{2,t}$ and their scaling coefficients $\mathcal{V}_{1,t}$ and $\mathcal{V}_{2,t}$ (k=0,…,N-1).

The Inverse DWT (IDWT) is achieved through upsampling the final level of wavelet and scaling coefficients, convolving them with their respective filters and adding up the two filtered vectors. Figure 2 gives a flow diagram for the reconstruction of X_t from the second level wavelet and scaling coefficient vectors. Given a dyadic length time series, it was not necessary to implement the DWT down to level $J = log_2(N)$. A partial DWT (PDWT) may be performed instead that terminates at a level $J_p < J$. The resulting vector of wavelet coefficients will then contain $N - N/2^{J_p}$ wavelets (Percival & Walden, 2000; Gencay et al., 2001). PDWT's are more commonly used in practice than the full DWT because of the flexibility they offer in specifying a scale beyond which a wavelet analysis

into individual large scales is no longer of real interest. A PDWT of level J_0 allows us to relax the restriction that N satisfy, $N = 2^J$ for some J and replace this restriction with the condition that N can be an integer multiple of 2^{J_0} (Percival & Walden, 2000; Gencay et al., 2001).
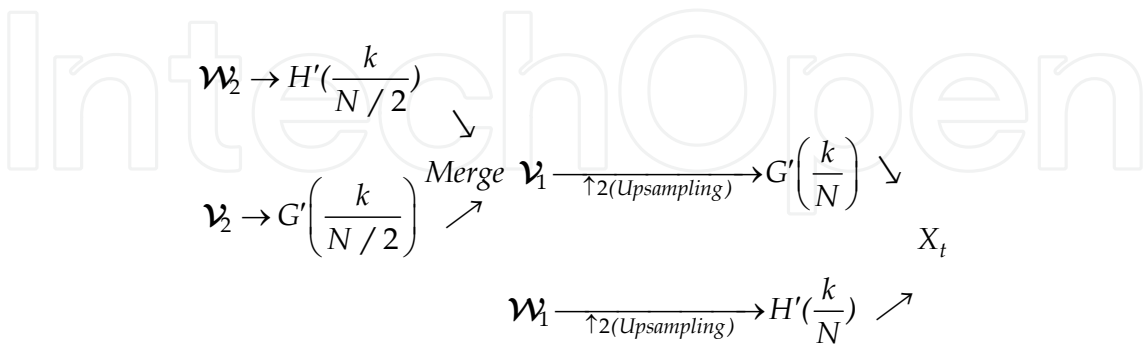
$$\mathcal{W}_2 \to H'(\frac{k}{N/2})$$
$$\mathcal{V}_2 \to G'\left(\frac{k}{N/2}\right) \quad Merge \quad \mathcal{V}_1 \xrightarrow[\uparrow 2 (Upsampling)]{} G'\left(\frac{k}{N}\right)$$
$$X_t$$
$$\mathcal{W}_1 \xrightarrow[\uparrow 2 (Upsampling)]{} H'(\frac{k}{N})$$

Fig. 2. Flow diagram illustrating the reconstruction of x_t^2 from first and second level wavelet coefficients $\mathcal{W}_{1,t}$ and $\mathcal{W}_{2,t}$ and their scaling coefficients $\mathcal{V}_{1,t}$ and $\mathcal{V}_{2,t}$ ($k=0,\ldots,N$-1).

2.2 The Maximal Overlap Discrete Wavelet (MODWT)

The DWT is an alternative to the Fourier transform (FT) for time series analysis. The DWT provides wavelet coefficients that are local in both time and frequency. In this section the maximal overlap DWT (MODWT) which is a modified version of the discrete wavelet transform is discussed. Like the DWT, the MODWT is defined in terms of a computationally efficient pyramid algorithm (PA). The term MODWT comes from the relationship of the MODWT with estimators of the Allan variance (Allan, 1966). The MODWT gives up orthogonality in order to gain features the DWT does not possess. A consequence of this is that the wavelet and scaling coefficients must be rescaled in order to retain the variance preserving property of the DWT (Percival & Guttorp, 1994).

Property	DWT	MODWT
Data	$N=2^J$	Any sample size N
Detail and Smooth Coefficients of MRA	Downsampling	Associated with zero phase filters
Circularly shifting	Does not hold	Holds and Invariant
Wavelet Variance	Less efficient	Asymptotically Efficient

Table 1. Properties of the DWT and MODWT

The properties in Table 1 are important in distinguishing the MODWT from the DWT (Percival & Mofjeld, 1997; Percival & Walden, 2000; Gencay et al., 2001). The decomposition and reconstruction procedure and inverting of the MODWT is similar to the DWT. A key feature to an MRA using the MODWT is that the wavelet details and smooth are associated

with zero-phase filters. Thus, interesting features in the wavelet details and smooth may be perfectly aligned with the original time series. This attribute is not available through the DWT since it subsamples the output of its filtering operations (Percival & Walden, 2000; Gencay et al., 2001).

2.3 Wavelet-based estimators of correlation

The length N vector of discrete wavelet coefficients W is obtained via $W = \mathcal{W}X$ and $W = \left[W_1, W_2, \cdots, W_J, V_J \right]^T$ where $\mathcal{W}$ is an $N \times N$ orthonormal matrix defining the DWT, W_j is a length $N/2^j$ vector of wavelet coefficients associated with changes on a scale of length $\lambda_j = 2^{j-1}$ and V_J is a length $N/2^J$ vector scaling coefficients associated with averages on a scale of length $2^J = 2\lambda_J$ in Section 2.1. Due to orthonormality, $X = \mathcal{W}^T W$, and the squared wavelet coefficients of W the norm, $\|W\|^2$, is the same as $\|X\|^2$ because of the equality $\|X\|^2 = X^T X = \left(\mathcal{W}^T W \right)^T \left(\mathcal{W}^T W \right) = W^T \mathcal{W}\mathcal{W}^T W = \|W\|^2$. Then $\|X\|^2$ can be decomposed on a scale-by-scale basis via $\|X\|^2 = \|W\|^2 = \sum_{j=1}^{J} \|W_j\|^2 + \|V_J\|^2$. The wavelet correlation and cross-correlation between two time series can now be defined. The wavelet correlation (WCORR) is the correlation between the scale λ_j wavelet coefficients of bivariate time series. Likewise the wavelet covariance is the covariance between the scale λ_j wavelet coefficients from bivariate time series. We introduce a lag τ, between the two series, to obtain the wavelet cross-covariance (WCCOVA) and wavelet cross-correlation (WCCORR) (Percival & Walden, 2000; Gencay et al., 2001), as described below.

Let X_t and Y_t be two time series of interest. The wavelet cross-covariance of (X_t, Y_t) for scale $\lambda_j = 2^{j-1}$ and lag τ is defined (Percival, 1995; Percival & Guttorp, 1994; Whitcher et al., 2000; Gencay et al., 2001) as follows,

$$\gamma_{\tau,XY}\left(\lambda_j \right) \equiv Cov\left\{ \overline{W}_{j,t}^X, \overline{W}_{j,t+\tau}^Y \right\} \tag{6}$$

where $\overline{W}_{j,t}^X$ and $\overline{W}_j^Y$ are the scale λ_j MODWT coefficients for X_t and Y_t. When the width of wavelet or scaling filter is equal or greater than two times of the number of differencing operations, the MODWT coefficients have mean zero and therefore the covariance reduces to an expectation of a product (Percival & Walden, 2000). By setting $\tau = 0$ and X_t to Y_t, $\gamma_{\tau,XY}\left(\lambda_j \right)$ reduces to the wavelet variance for X_t or Y_t denoted by $\sigma_X^2\left(\lambda_j \right)$ or $\sigma_Y^2\left(\lambda_j \right)$. The wavelet correlation of (X_t, Y_t) at scale $\lambda_j = 2^{j-1}$ is then defined as follows,

$$\rho_{XY}\left(\lambda_j \right) = \frac{Cov\left\{ \overline{W}_{j,t}^X, \overline{W}_{j,t}^Y \right\}}{\sigma_X\left(\lambda_j \right).\sigma_Y\left(\lambda_j \right)} = \frac{\gamma_{XY}\left(\lambda_j \right)}{\sigma_X\left(\lambda_j \right).\sigma_Y\left(\lambda_j \right)}. \tag{7}$$

Rationale for wavelets	**Qualitative Description of the DWT and MODWT**
Wavelets allow time series data to be decomposed on a scale by scale basis, or to be discretized, into its so-called underlying subcomponents. Conventional time frequency domain methods results may be difficult to interpret, whereas the wavelet-correlation is able to display how the association between two time series change with wavelet scale. Transformation of the data (orthonormal) allows correlation, cross-correlational analyses of bivariate series to be performed - based on the derived wavelet coefficients. DWT is often less computer intensive than other transformations (e.g. fast Fourier transform). DWT offers easier analysis than the CWT as most time series are sampled as discrete values. DWT allows for the decorrelation of time series.	DWT transforms the original time series X into its DWT coefficients $W = wY$, where w is a $N \times N$ orthonormal matrix − the components, W_j, of W are associated with coefficients for each scale $\lambda_j = 2^{j-1}$ Wavelet coefficients Wj inform on the variations in adjacent averages over λ_j. There are $\dfrac{N}{2\lambda_j}$ wavelet coefficients for each scale $\lambda_j \equiv 2^{j-1}$, j = 1, 2 . . , J_0 where $\lambda_j = 2^{j-1}$ is a so-called standardized scale, whereas $\lambda_j \Delta t$ is a physical scale, where Δt is the sampling interval. The MODWT is a non-decimated variation of the DWT, which defines the jth level MODWT detail subcomponent of the time series as $\overline{D}_j = \overline{W}_j^T \overline{W}_j$ and defines the jth level MODWT smoothed series, $\overline{S}_j = \overline{V}_j^T \overline{V}_j$, which is related to the average (over scale N), and is normally interpretable as the trend.
Cross- Correlation and correlation The scale λ_j MODWT coefficients may be used to investigate the correlation and cross-correlation of two time series, X_t and Y_t. The wavelet cross correlation of X_t, Y_t at scale $\lambda_j=2^{j-1}$ for a time lag τ, is defined as $\rho_{XY,\tau}(\lambda_j) = \dfrac{Cov\left\{\overline{W}_{j,t}^X \overline{W}_{j,t}^Y\right\}}{\sigma_X(\lambda_j)\cdot\sigma_Y(\lambda_j)} = \dfrac{\gamma_{XY,\tau}(\lambda_j)}{\sigma_X(\lambda_j)\cdot\sigma_Y(\lambda_j)}$, where $\overline{W}_{j,t}^X$ and $\overline{W}_{j,t}^Y$ are scale λ_j MODWT coefficients. Correlation is the cross-correlation at lag $\tau = 0$.	**MODWT-MRA** The orthonormal matrix, $N \times N$, leads to scale-based decompositions. Given the MODWT coefficients, Y can be constructed as an additive decomposition, known as a multiresolution analysis (MRA). Specifically the level J_0 MODWT-based MRA is given by $Y = \sum_{j=1}^{J_0} \overline{d}_j + \overline{s}_{j0}$, $\overline{d}_j$ are the "detail series", ($j= 1, 2, . . ., J_0$) for a pre- specified J_0, and are part of the MRA of Y that can be attributed to variations on a scale of λ_j.

Table 2. Summary of the wavelet mathematics and rationale.

where $\sigma_X^2\left(\lambda_j\right) = var\left\{\overline{W}_{j,t}^{X}\right\}$ is the wavelet variance with scale λ_j. $\overline{W}_{j,t}^{X}$ and $\overline{W}_{j,t}^{Y}$ are the scale λ_j MODWT coefficients for X_t and Y_t, respectively (Percival & Walden, 2000; Gencay et al., 2001). As with the usual correlation coefficient (between two random variables), the range of $\rho_{XY}\left(\lambda_j\right)$ is the interval –1 to 1 for all j. The typical cross-correlation statistic is purely a function of the cross-covariance and standard deviations. Thereby the MODWT estimator of the wavelet cross-correlation (WCCORR) of the two processes, which are at variance by an integer lag τ, is defined as

$$\rho_{XY,\tau}\left(\lambda_j\right) = \frac{Cov\left\{\overline{W}_{j,t}^{X}, \overline{W}_{j,t}^{Y}\right\}}{\sigma_X\left(\lambda_j\right).\sigma_Y\left(\lambda_j\right)} = \frac{\gamma_{XY,\tau}\left(\lambda_j\right)}{\sigma_X\left(\lambda_j\right).\sigma_Y\left(\lambda_j\right)} . \tag{8}$$

As the usual cross-correlation is used to determine lead or lag relationships between two series, the wavelet cross-correlation provides a lead or lag relationship between X_t and Y_t on a scale-by-scale basis. In terms of confidence intervals (CIs) for the WCORR and WCCORR parameters, a nonlinear transformation is required to produce reasonable CIs for the correlation coefficient (Gencay et al., 2001). We use the Fisher's z-transformation (Dépué 2003) which is defined as follows,

$$h\left(\rho\right) = \frac{1}{2}log\left(\frac{1+\rho}{1-\rho}\right) = tanh^{-1}\left(\rho\right). \tag{9}$$

An unbiased estimator of the WCORR based on the MODWT in Equation (7) is $\tilde{\rho}$. The given estimated correlation coefficient $\tilde{\rho}$, based on N independent Gaussian observations, has the following limiting distribution (Percival & Walden, 2000; Gencay et al., 2001).

$$\sqrt{N-3}\left[h(\tilde{\rho}) - h(\rho)\right] \sim N\left(0,1\right). \tag{10}$$

Applying the transformation tanh maps the confidence interval back to [−1, 1] to produce an approximate 95% CI for ρ as follows (Whitcher et al. 2000; Gencay et al. 2001; Hudson et al., 2010b)

$$tanh\left\{h\left[\tilde{\rho}_{XY}\left(\lambda_j\right)\right] \pm \zeta_{\frac{\alpha}{2}}\left(\frac{1}{\hat{N}_j - 3}\right)^{1/2}\right\}. \tag{11}$$

The quantity $\hat{N}_j$ in Equation (11) is the number of the DWT coefficients associated with scale λ_j. Table 2 gives a brief overview of the wavelet mathematics used in this chapter.

3. Application to Agitation Sedation (A-S) wavelet modelling

This section presents the application of a wavelets analysis of the agitation-sedation (A-S) data of 37 ICU patients' bivariate time series, sourced from the research of Chase et al. (2004). An extensive description of A-S modelling, as well as other references on A-S control;

along with details of the development and validation of the A-S model are given in Chase et al. (2004). The model by Chase et al. (2004) serves as a platform to develop and test semi-automated sedation management controllers that offer the potential of improved agitation management and reduced length of stay in the ICU. Figure 3 presents a diagram of the feedback loop employing nursing staff feedback of subjectively assessed patient agitation through the infusion controller (Chase et al., 2004). We refer the reader also to the later works of Lee et al. (2005) and of Rudge et al. (2005, 2006a, 2006b) who developed further A-S models and metrics. Table 3 summarises the equations used, mathematical methods employed and the aims of the given study, along with the performance indicators derived for each of Chase et al. (2004), Rudge et al. (2006a, 2006b, 2005), and Lee et al. (2005). As such Table 3 and subsequently Table 8 show how the research presented in this chapter adds knowledge and insight into A-S modelling in the context of these earlier works.

3.1 Using the DWT and MODWT

The DWT, the maximal overlap (MODWT) and multiresolution analysis (MRA) were applied to all pairs of patient specific infusion profiles (recorded (R) and simulated (S)) for the 37 ICU patients. The aim of the analysis reported in section 3.1 – 3.3 is to investigate
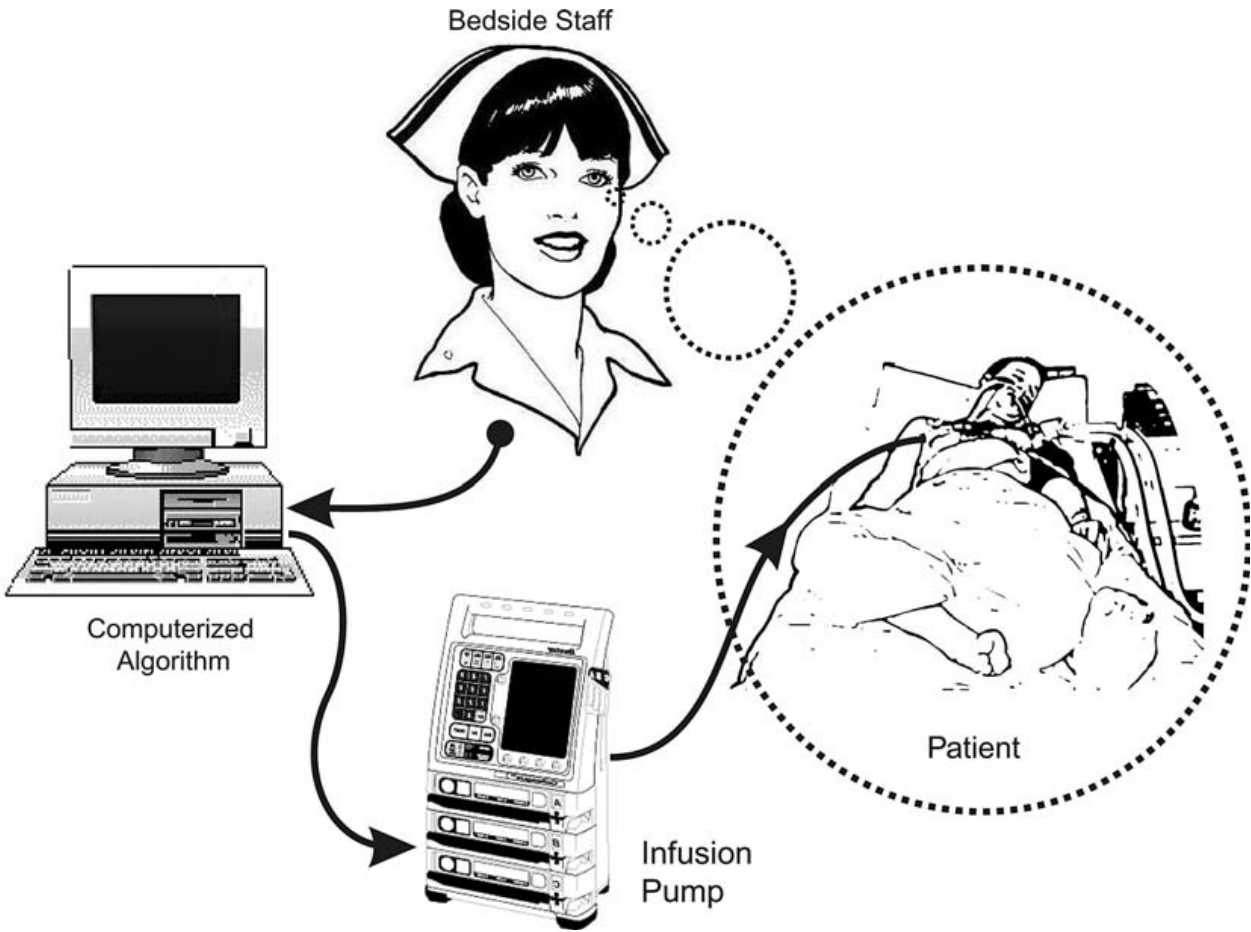

Fig. 3. Diagram of the feedback loop employing nursing staff feedback of subjectively assessed patient agitation through the infusion controller (diagram is sourced from Chase et al. (2004)).

whether wavelets based diagnostics can reliably assess how well the A-S model (simulation) captures the underlying dynamics of the true recorded infusion rates at different horizons via the DWT; and to compare these results with the diagnostics of Chase et al. (2004), Rudge et al. (2006a, 2006b, 2005) and Lee et al. (2005). For illustration of these concepts patient specific recorded (R) and simulated (S) profiles (as the thick line, according to the equation of Chase et al. (2004)) are shown in Figure 4. It is noteworthy that simulation of the A-S states using the model of Rudge et al. (2005) showed that a reduction in both the magnitude of agitation and the severity of agitation sedation cycling is possible. Mean and peak agitation levels were reduced by 68.4% and 52.9%, respectively, on average, with some patients exhibiting in excess of a 90% reduction in mean agitation level through increased control gains. Implementation of automated feedback infusion controllers based on such models could thus offer simple and effective drug delivery, without significant increases in drug consumption and expenses.

The lag/lead relationship between the S and R infusion series was investigated on a scale-by-scale basis via a MODWT-MRA (using the LaDaub (8) filter); thereby each patient's S and R series can be expressed as a new set of series, called details and smooth. Each of these series are associated with variations at a particular wavelet scale. The results of a MODWT-MRA (not detailed here due to space restrictions) reveal that thirteen patients (patients 3, 9, 11, 17, 20, 22, 26, 30, 33, 34, 35, 36, 37) (Figure 4) have recorded infusion series that lead their corresponding simulated infusion series. It is noteworthy that of these 13 patients, which exhibit such a lagged dependency, our DWT wavelet diagnostics (and those of Chase et al., (2004) and Rudge et al., (2006b)) identify the following as poor performers in common (Patients 9, 11, 17, 22, 33, 34 and 35). Overall it is thought that the simulated profile peaks later than the patient's recorded infusion possibly due to the delay in distribution time for the drug. This result implies that, while performing well most of the time, the simulated rate is lagging behind the patient's true infusion rate. These periods indicate times of the patient's hospital length of stay in ICU, where the DE model may not capture the subject's specific A-S dynamics (evidenced by the time lags). These periods may correspond to periods of marked distress or physiological alterations due to the patient's state. A common reason for the departure of the simulated profile is this apparent time-lag. Particularly small departures indicate rapid increases (or decreases) in the recorded infusion rate, where the simulated infusion rate appears to lag behind. These differences may be a result of the medical staff's over or under-assessment of the patient's agitation status, this hypothesis is as yet not proven.

3.2 Wavelet correlation and other diagnostics

In section 3.2 an estimate of wavelet correlation (WCORR), $\tilde{\rho}$ from Equation (7), is derived per patient. This WCORR between the scale λ_j wavelet coefficients of each patient's bivariate (S, R) time series is used to assess how the simulated (S) and recorded (R) infusion series correlate. Graphical assessment tools and derived wavelet-based metrics are then suggested and proven valid for ICU A-S management. The wavelets based performance indices developed in this chapter pertain to the modulus of the wavelet correlation at wavelet scale (λ_j) (level 1) and also to summary statistics founded on measures of the wavelet correlations and wavelet cross-correlations over scales, as defined below (Table 6). For the ith patient (i=1, 2, …, 37) count the number of its wavelet scales (out of a maximum of 8) for which the WCORR value at scale λ_j is not significant (at the 5% level of significance). This variable is

denoted by "Count of NS" and given per patient, with specification of the significance (at the 5% level of significance) of WCORR at λ_j (j=1, 2, …, 8) as either significant (S) or not significant (NS) in Table 4. Patient specific AND (average normalized density), RAND (relative average normalized density), and TI (tracking index) values, all derived by Rudge et al (2006b) and Chase et al. (2004), are also shown in Table 4. Definitions for the AND, RAND and TI performance indicators or diagnostics are detailed in Table 3.
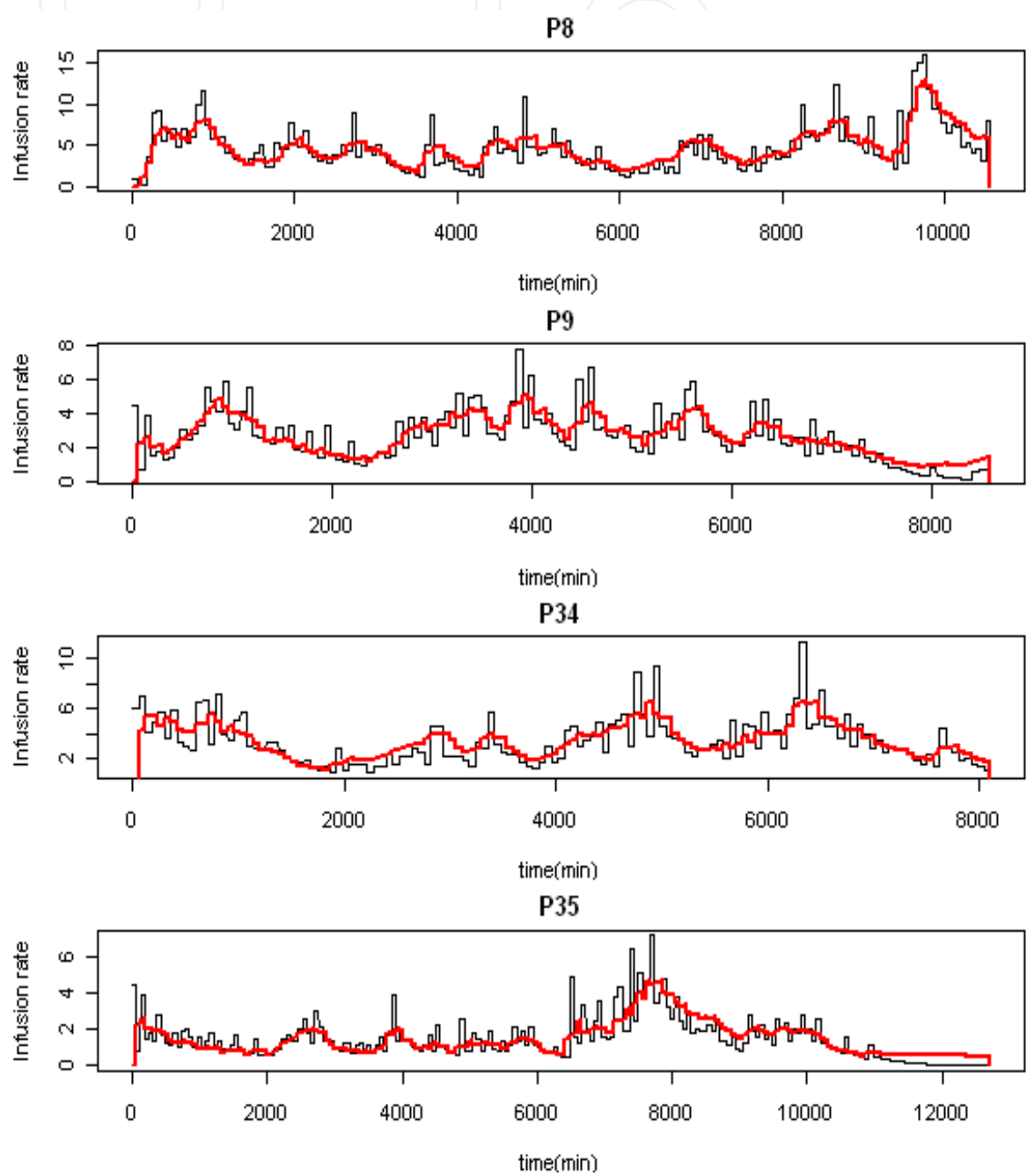

Fig. 4. Example of the delay between the recorded and simulated (thick line) infusion profiles for Patients 8, 9, 34 and 35 (denoted by P8, P9, P34 and P35). P8 is shown to be a good tracker, the remainder are poor trackers, according to the indices developed in this chapter.

Authors	Equations or Model used	Mathematical methods used	Aims of the study and the performance indicators derived
Rudge et al. (2006 a, b)	I. Pharmacokinetics of morphine : $$V_c^o \frac{dC_c^o}{dt} = -\left(K_{CL}^o + K_{ce}^o + K_{cp}^o\right)C_c^o + P^o U + K_{ec}^o C_e^o + K_{pc}^o C_p^o$$ $$V_p^o \frac{dC_p^o}{dt} = -K_{pc}^o C_p^o + K_{cp}^o C_c^o , V_e^o \frac{dC_e^o}{dt} = -K_{ec}^o C_e^o + K_{ce}^o C_c^o$$ II. Pharmacodynamics of midazolam : $$V_c^s \frac{dC_c^s}{dt} = -\left(K_{CL}^s + K_{ce}^s\right)C_c^s + P^s U + K_{ec}^s C_e^s , V_e^s \frac{dC_e^s}{dt} = -K_{ec}^s C_e^s + K_{ce}^s C_c^s$$ III. Pharmacodynamics of morphine and midazolam : $$\frac{dA}{dt} = w_1 S - w_2 K_T \int_0^t E_{comb}(\zeta) e^{-K_T(t-\zeta)} d\zeta , E_{Comb} = E_0 + \left[E_{max}(\theta) - E_0\right] \frac{\left(\frac{C_o + C_S}{C_{50}(\theta)}\right)^{\gamma(\theta)}}{1 + \left(\frac{C_o + C_S}{C_{50}(\theta)}\right)^{\gamma(\theta)}}$$	Kernel smoothing Chebychev's inequality for probability band (Chase et al., 2004) Relative average normalised density (RAND) Average normalised density (AND)	Develop a physiologically representative that incorporates endogenous ag reduction (EAR). Use performance measures as follows: 1. RTD: relative total dose (RTD) exp the total dose administered i simulation as a percentage of the total recorded dose. 2. Relative average normalised (RAND) measures how probabilis similar the model outputs are smoothed data, and hence the deg comparability between the model a empirical data. 3. Percentage time in band (TIB).
Rudge et al. (2005)	I. Pharmacokinetics of morphine : $$V_c^o \frac{dC_c^o}{dt} = -\left(K_{CL}^o + K_{ce}^o + K_{cp}^o\right)C_c^o + P^o U + K_{ec}^o C_e^o + K_{pc}^o C_p^o$$ $$V_p^o \frac{dC_p^o}{dt} = -K_{pc}^o C_p^o + K_{cp}^o C_c^o , V_e^o \frac{dC_e^o}{dt} = -K_{ec}^o C_e^o + K_{ce}^o C_c^o$$ II. Pharmacodynamics of midazolam : $$V_c^s \frac{dC_c^s}{dt} = -\left(K_{CL}^s + K_{ce}^s\right)C_c^s + P^s U + K_{ec}^s C_e^s , V_e^s \frac{dC_e^s}{dt} = -K_{ec}^s C_e^s + K_{ce}^s C_c^s$$ III. Pharmacodynamics of morphine and midazolam : $$\frac{dA}{dt} = w_1 S - w_2 K_T \int_0^t E_{comb}(\zeta) e^{-K_T(t-\zeta)} d\zeta , E_{Comb} = E_0 + \left[E_{max}(\theta) - E_0\right] \frac{\left(\frac{C_o + C_S}{C_{50}(\theta)}\right)^{\gamma(\theta)}}{1 + \left(\frac{C_o + C_S}{C_{50}(\theta)}\right)^{\gamma(\theta)}}$$	Infinite Impluse Response (IIR) filter (Rorabaugh, 1998) Proportional-Derivative (PD) control with agitation for infusion rate (U) Moving blocks bootstrap (Efron & Tibshirani, 1993) Tracking Index (TI)	Develop a control model to capture the es dynamics of the agitation-sedation system Use performance measures as follows: 1. $U = K_p A + K_d A$ for the infusion rate. 2. Tracking Index (TI): A quantitative para to indicate how well the sim infusion profile represents the a recorded infusion.

Table 3. Overview of Agitation-Sedation studies of ICU patients.

Authors	Equations or Model used	Mathematical methods used	Aims of the study and the performance indicators derived
Lee et al. (2005)	I. Pharmacokinetics of morphine : $$V_c^o \frac{dC_c^o}{dt} = -\left(K_{CL}^o + K_{ce}^o + K_{cp}^o\right)C_c^o + P^o U + K_{ec}^o C_e^o + K_{pc}^o C_p^o$$ $$V_p^o \frac{dC_p^o}{dt} = -K_{pc}^o C_p^o + K_{cp}^o C_c^o, \quad V_e^o \frac{dC_e^o}{dt} = -K_{ec}^o C_e^o + K_{ce}^o C_c^o$$ II. Pharmacodynamics of midazolam : $$V_c^s \frac{dC_c^s}{dt} = -\left(K_{CL}^s + K_{ce}^s\right)C_c^s + P^s U + K_{ec}^s C_e^s, \quad V_e^s \frac{dC_e^s}{dt} = -K_{ec}^s C_e^s + K_{ce}^s C_c^s$$ III. Pharmacodynamics of morphine and midazolam : $$\frac{dA}{dt} = w_1 S - w_2 K_T \int_0^t E_{comb}(\zeta) e^{-K_T(t-\zeta)} d\zeta, \quad E_{Comb} = E_0 + \left[E_{max}(\theta) - E_0\right]\frac{\left(\frac{C_o + C_S}{C_{50}(\theta)}\right)^{\gamma(\theta)}}{1 + \left(\frac{C_o + C_S}{C_{50}(\theta)}\right)^{\gamma(\theta)}}$$	Kernel regression (Wand & Jones, 1995) Kernel density estimation: marginal density function of the regression function estimate Nonparametric regression Chebychev's inequality for the probability band (Chase et al., 2004)	Develop a nonparametric approach for assessing the validity of deterministic dynamic models against empirical data. Use performance measures as follows: 1. Kernel regression and kernel d estimation to yield visual gra assessment of the data. 2. Construct a probability band f nonparametric regression curve check whether the proposed mod within the band, for a sign proportion of the time. 3. Average normalised density (AN measure how well the simulated coincide with the maximum den every time point and the r average normalised density (RAN
Chase et al. (2004)	The agitation-sedation system model: Pharmacokinetic model (Wood & Wood, 1990) adding patient agitation as a third state variable $$\frac{dC_c}{dt} = -K_1 C_c + \frac{U}{V_d}$$ $$\frac{dC_p}{dt} = -K_2 C_p + K_3 C_c$$ $$\frac{dA}{dt} = w_1 S - w_2 \int_0^t C_p(\tau) e^{-K_4(t-\tau)} d\tau$$ Uniform kernel with bandwidth h (Wand & Jones, 1995) $$K_h = \begin{cases} 0 & \text{if } t < -\frac{h}{2} \\ 1 & \text{if } -\frac{h}{2} < t \leq \frac{h}{2} \\ 0 & \text{if } t > \frac{h}{2} \end{cases}$$	Infinite Impulse Response (IIR) filter (Rorabaugh, 1998) Proportional-Derivative (PD) control with agitation for infusion rate (U) Tracking Index (TI) Chebychev's inequality for the probability band (Chase et al., 2004)	Develop a mathematical model to captu essential dynamics of the agitation-se system and develop statistical validity using the recorded infusion data for 3 patients. Use performance measures as follows 1. Kernel smoothing using the u kernel. 2. Tracking Index (TI). 3. Moving blocks bootstrap to ga understanding of the reliability T given patient's infusion profile 4. 90% Probability Band, by definiti range within at least 90% of the the estimated mean value o recorded infusion rate lies with band.

From Lee et al (2005) and Chase et al (2004): "Po and Ps are the concentrations of morphine and midazolam, re terms with superscript 'o' relate to the opioid morphine, and terms with superscript 's' relate to the sedative m by t (min), the variable of integration, and the terms w1 and w2 are the relative weights of stimulus and cumu patient sensitivity. Finally, Ecomb is the combined pharmacodynamic effect of the individual effect site drug c midazolam determined using response surface modeling as defined in Minto et al. (Minto et al., 2000)."

Poor trackers are identified via wavelet diagnostics as follows: Patients with a "Count of NS" greater or equal to 2 and a non-significant WCORR value at scale λ_1 (level 1) are said to be a poor tracker; as are patients with a "Count of NS" less or equal to 3 and a *significant negative* WCORR value at scale λ_1 (level 1) and a *significant negative* WCORR value at scale λ_6. Table 4 indicates 15 such poor trackers (given in bold), as defined by the wavelet based diagnostics ("Count of NS" and WCORR at scales λ_1 and λ_6) derived in this chapter. Poor tracking implies that the patient's simulated A-S profiles do not mirror their actual (recorded) infusion profile over time (according to their profile of wavelet correlations).

Note that the threshold values delineating poor tracking for AND and RAND (according to Rudge et al. (2006b)) are not taken into account in classifying a patient as either a poor or good tracker (Table 4). In this chapter our criterion for tracking classification is based solely on the patient's WCORR values at scales λ_j (j=1, 2, …, 8), their significance or otherwise, and on their "Count of NS" wavelet correlations (Table 4). As mentioned above Table 4 also indicates patients which are considered to track poorly according to both Rudge et al's (2006b) and Chase et al.'s (2004) diagnostics, the latter are based on completely different mathematical methodologies as summarised in Table 3. It is noteworthy that 11 of our 15 wavelet based poor trackers are also considered to be poor trackers by either or both of Rudge et al.'s (2006b) and Chase et al.'s (2004) performance indices.

Figure 5 shows the estimated WCORR, $\tilde{\rho}$ and 95% CI for four patients, P2 and P4 (are poor trackers) and P8 and P14 (are good trackers). From Figure 5 WCORR is generally significant for wavelet levels 1, 2, 4, 8 and 16 for the good trackers (whether they are a positive or negative WCORR value). This is not the case for the poor trackers, who generally exhibit a non-significant WCORR at λ_j for j < 5. Figures 6 and 7 display each patient's multivariate profile of AND, RAND and "Count of NS" (divided by 10 for axis scaling purposes), for increasing $|\lambda_1|$, for the poor trackers and good trackers, respectively. Figures 6-7 clearly show that the profile of ("Count of NS"/10) is invariably higher for the poor trackers; and RAND, AND and $|\lambda_1|$ profiles are invariably higher for the good trackers.

By using the data per patient (from Table 4), we can perform a Kruskal Wallis test to statistically compare the medians of the performance indicators between the wavelet based good and poor trackers. These results are summarized in Table 5 and Table 6. Specifically Table 6 gives the results of the Kruskal Wallis (k-w) tests for our wavelet based poor versus good tracker groups for measures of WCORR at scale λ_j (j=1, 2, …, 8), "Count of NS", $|\lambda_1|$, in addition to AND, RAND and TI per patient. From Table 6 we observe that the median wavelet correlations for the first 5 wavelet scales are significantly lower for the poor trackers (15 of 37 patients), as are the median absolute value of the wavelet correlation at λ_1, and of AND, RAND and TI (P < 0.006). The median of the number of non significant wavelet correlations ("Count of NS") (an integer out of 8, at λ_j, j=1, 2,…, 8) is 5.0 for the poor trackers, significantly higher than the median of 2.0 for the good tracking group (P = 0.001) (Table 6). It is noteworthy also that the patient specific WCORR profiles are good visual "signatures" of the patient's tracking status (good or poor tracking) (see Figure 5).

Recall that 11 of the 15 DWT based poor trackers are also considered to be poor trackers by either or both Rudge et al.'s (2006b) and Chase et al.'s (2004) (non wavelet based) performance indicators. Indeed kappa tests of agreement show that our DWT WCORR

criterion for poor tracking, as developed in this chapter, agrees significantly with that of the performance thresholds of Chase et al (2004) (*kappa* = 0.2127, P=0.01) and with that of Rudge et al. (2006b) (*kappa* = 0.5856, P=0.001). It is noteworthy also that the threshold criterion for poor tracking for RAND by both Rudge et al.'s (2006b) and Chase et al.'s (2004) performance indicators is corroborated by our poor trackers, identified by the wavelet metrics derived in this chapter, shown to have a median RAND of 0.50 (Table 6), which is exactly the threshold used by Rudge et al. (2006b) and Chase et al. (2004).
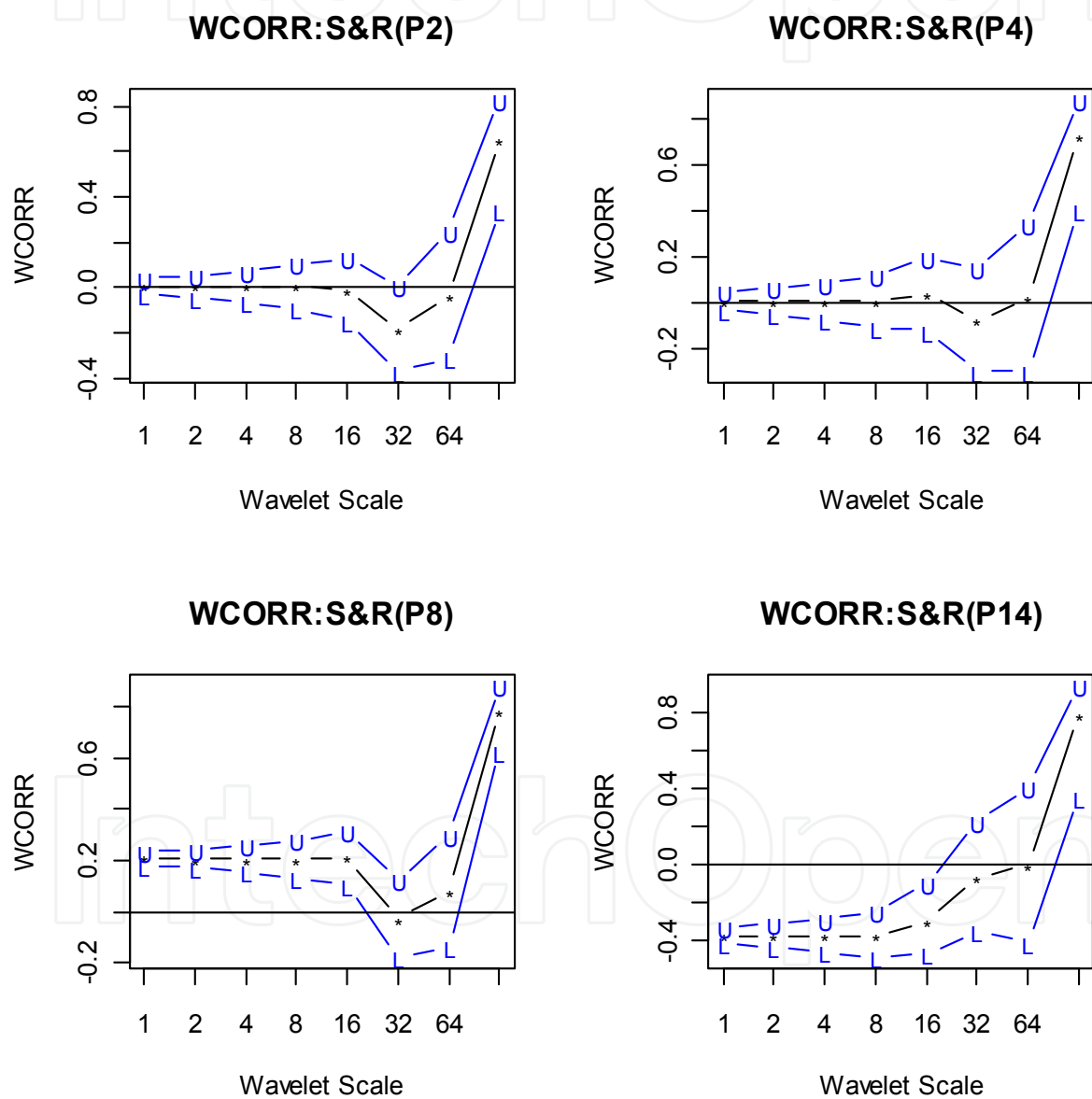
Fig. 5. Wavelet correlation for Patient 2 (Top LHS), Patient 4 (Top RHS), Patient 8 (bottom LHS) and Patient 14 (bottom RHS) with the approximate 95% confidence interval. Patients 2 and 4 are poor trackers in contrast to Patients 8 and 14 who are good trackers with >4 significant WCORR at wavelet scales (1, 2, 4, 8, 16).
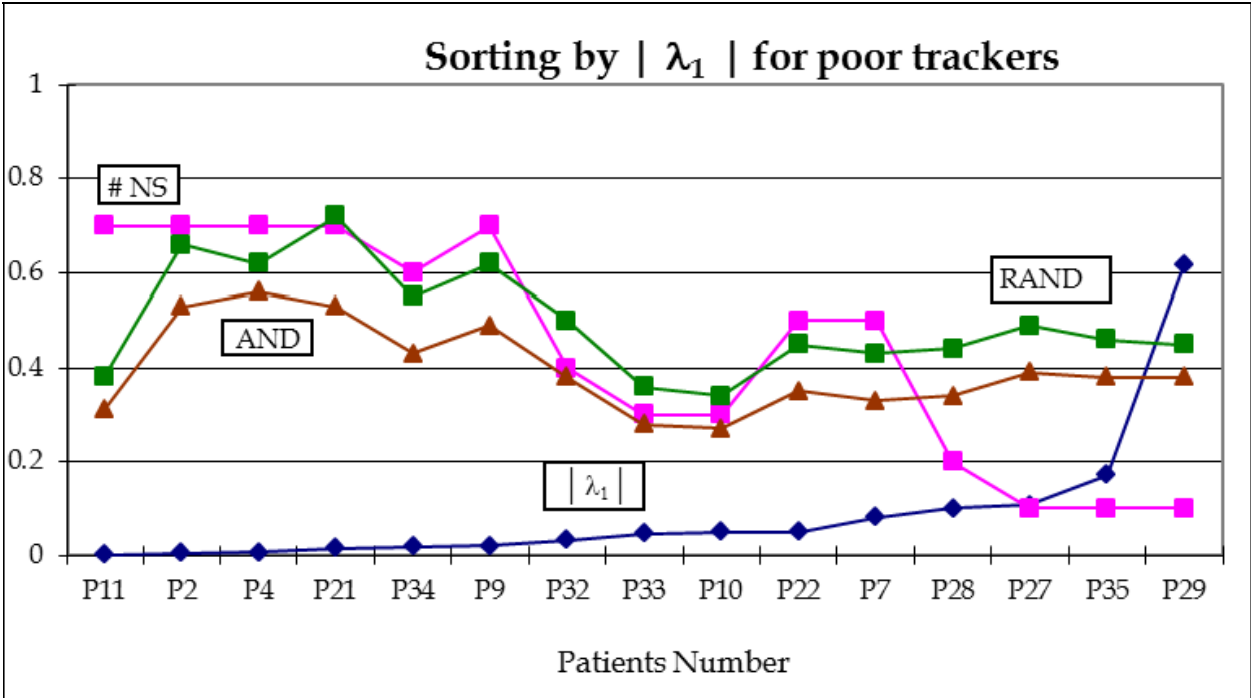
Fig. 6. A comparison of RAND (green square), AND (burgundy triangle), the number of non-significant λ_j (divided by 10) (pink square), and the modulus of λ_1 (blue diamond) for the poor trackers (P11, P2,…, P29) sorted by increasing $|\lambda_1|$.

Fig. 7. A comparison of RAND (green square), AND (burgundy triangle), the number of non- significant λ_j (divided by 10) (pink square), and the modulus of λ_1 (blue diamond) for the good trackers (P31, P30,..., P3) sorted by increasing $|\lambda_1|$.

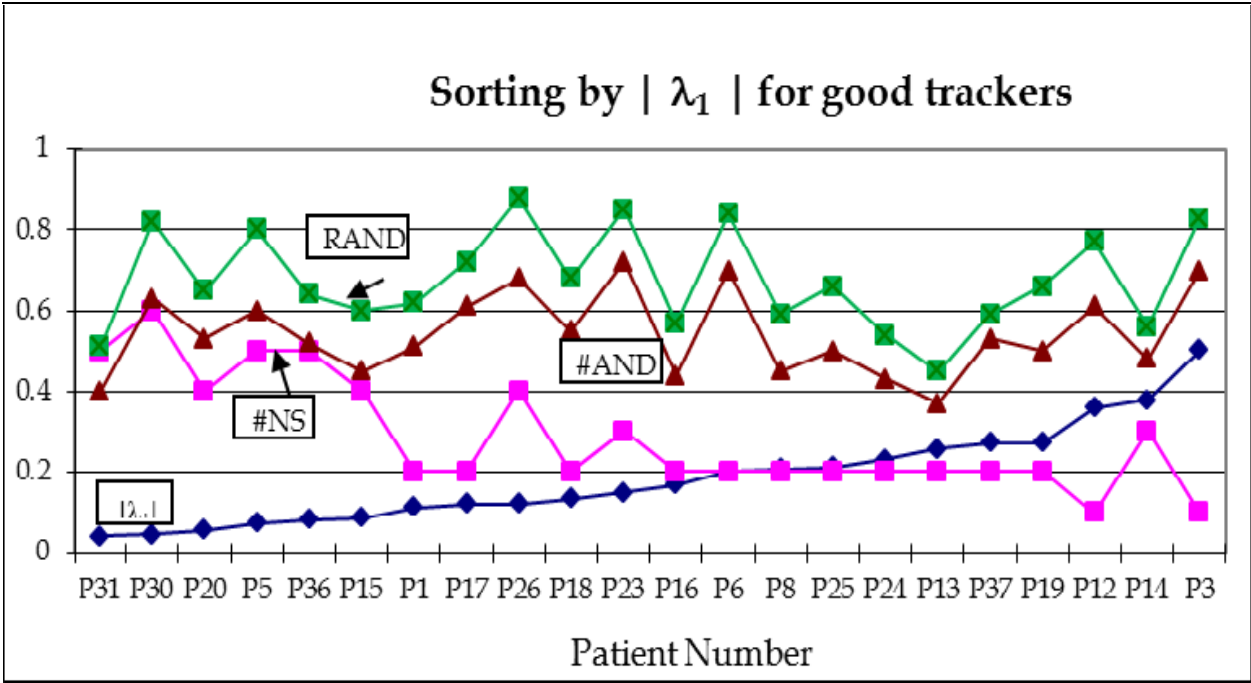| Patient ID	Wavelet scale λ_j (j= 1, 2, …, 8)								Count of NS*	Rudge et al. (2006b) diagnostics		Chase et al. (2004) diagnostics
	1	2	4	8	16	32	64	128		AND·	RAND·	TI (SE)·
P1	S	S	S	S	S	NS	NS	S	2	0.51	0.62	87.0 (0.041)
P2	NS	NS	NS	NS	NS	NS	NS	S	7	0.53	0.66	86.2 (0.037)
P3	S	S	S	S	S	S	N.S	S	1	0.70	0.83	88.8 (0.015)
P4	NS	NS	NS	NS	NS	NS	NS	S	7	0.56	0.62	80.1 (0.095)
P5	S	S	NS	NS	NS	NS	NS	S	5	0.60	0.80	91.1 (0.016)
P6	S	S	S	S	S	NS	NS	S	2	0.70	0.84	87.0 (0.014)
P7	S	S	NS	NS	NS	NS	NS	S	5	0.33	0.43	84.5 (0.068)
P8	S	S	S	S	S	NS	NS	S	2	0.45	0.59	87.4 (0.027)
P9	NS	NS	NS	NS	NS	NS	NS	S	7	0.49	0.62	87.3 (0.024)
P10	S	S	S	NS	NS	S	NS	S	3	0.27	0.34	83.4 (0.041)
P11	NS	NS	NS	NS	NS	NS	NS	S	7	0.31	0.38	83.7 (0.080)
P12	S	S	S	S	S	S	NS	S	1	0.61	0.77	84.1 (0.033)
P13	S	S	S	S	S	NS	NS	S	2	0.37	0.45	86.1 (0.072)
P14	S	S	S	NS	S	NS	NS	S	3	0.48	0.56	93.1 (0.034)
P15	S	S	S	NS	NS	NS	NS	S	4	0.45	0.60	91.1 (0.011)
P16	S	S	S	S	S	NS	NS	S	2	0.44	0.57	87.9 (0.021)
P17	S	S	S	S	S	NS	NS	S	2	0.61	0.72	84.0 (0.037)
P18	S	S	S	S	NS	S	NS	S	2	0.55	0.68	94.6 (0.026)
P19	S	S	S	S	S	NS	NS	S	2	0.50	0.66	91.1 (0.014)
P20	S	S	S	NS	NS	NS	NS	S	4	0.53	0.65	87.3 (0.033)
P21	NS	NS	NS	NS	NS	NS	NS	S	7	0.53	0.72	78.5 (0.095)
P22	S	S	NS	NS	NS	NS	NS	S	5	0.35	0.45	85.2 (0.043)
P23	S	S	S	S	NS	NS	NS	S	3	0.72	0.85	84.8 (0.105)
P24	S	S	S	S	S	NS	NS	S	2	0.43	0.54	88.1 (0.023)
P25	S	S	S	S	S	NS	NS	S	2	0.50	0.66	92.4 (0.025)
P26	S	S	S	NS	NS	NS	NS	S	4	0.68	0.88	87.4 (0.031)
P27	S	S	S	S	NS	S	S	S	1	0.39	0.49	74.9 (0.074)

Patient ID	Wavelet scale λ_j (j= 1, 2, …, 8)								Count of NS*	Rudge et al. (2006b) diagnostics		Chase et al. (2004) diagnostics
	1	2	4	8	16	32	64	128		AND·	RAND·	TI (SE)·
P28	S	S	S	S	NS	S	NS	S	2	0.34	0.44	89.2 (0.027)
P29	**S**	**S**	**S**	**S**	**S**	**S**	**NS**	**S**	**1**	**0.38**	**0.45**	**77.6 (0.083)**
P30	NS	NS	NS	NS	NS	NS	S	S	6	0.63	0.82	92.2 (0.021)
P31	S	S	NS	NS	NS	NS	NS	S	5	0.40	0.51	89.3 (0.030)
P32	S	S	NS	NS	NS	S	NS	S	4	0.38	0.50	89.3 (0.022)
P33	**S**	**S**	**S**	**NS**	**NS**	**S**	**NS**	**S**	**3**	**0.28**	**0.36**	**88.7 (0.020)**
P34	NS	NS	NS	NS	NS	S	NS	S	6	0.43	0.55	86.5 (0.034)
P35	**S**	**S**	**S**	**S**	**S**	**S**	**NS**	**S**	**1**	**0.38**	**0.46**	**85.9 (0.044)**
P36	S	S	NS	NS	NS	NS	NS	S	5	0.52	0.64	86.4 (0.095)
P37	S	S	S	S	S	NS	NS	S	2	0.53	0.59	79.9 (0.093)

Table 4. Wavelet correlation analysis of the 37 ICU patients. S-significant, NS-non-significant WCORR at given scale λ_j (j= 1, 2, …, 8). Bolded patients indicate poor trackers according to the WCORR and "Count NS" values. Patient 30 has NS=6, which is large, but their high AND=0.63, RAND=0.82, and TI=92.2% are indicative of good tracking.

Poor Patient ID	Wavelet Correlations (scale λ_j)								Rudge et al. (2006b) diagnostics		Chase et al. (2004) diagnostics
	λ_1	λ_2	λ_3	λ_4	λ_5	λ_6	λ_7	λ_8	AND	RAND	TI(SE)
P2	0.005	0.005	0.005	0.005	-0.008	-0.186	-0.034	0.649	0.53	0.66	86.2 (0.03)
P4	0.006	0.006	0.005	0.005	0.036	-0.077	0.023	0.724	0.56	0.62	80.1 (0.09)
P7	-0.081	-0.081	-0.081	-0.081	-0.037	-0.066	0.034	0.785	0.33	0.43	84.5 (0.06)
P9	-0.020	-0.021	-0.021	-0.021	0.012	-0.066	0.012	0.793	0.49	0.62	87.3 (0.02)
P10	0.051	0.051	0.051	0.051	0.052	-0.125	-0.040	0.591	0.27	0.34	83.4 (0.04)
P11	-0.001	-0.001	-0.001	-0.001	0.019	0.093	0.002	0.654	0.31	0.38	83.7 (0.08)
P21	0.016	0.017	0.017	0.017	0.026	-0.148	-0.031	0.779	0.53	0.72	78.5 (0.09)
P22	-0.051	-0.051	-0.051	-0.051	-0.027	-0.115	-0.052	0.739	0.35	0.45	85.2 (0.04)
P27	-0.108	-0.108	-0.108	-0.108	-0.088	-0.227	-0.201	0.660	0.39	0.49	74.9 (0.07)
P28	-0.100	-0.101	-0.101	-0.101	-0.090	-0.200	-0.157	0.628	0.34	0.44	89.2 (0.02)
P29	-0.616	-0.616	-0.616	-0.616	-0.582	-0.497	-0.294	0.627	0.38	0.45	77.6 (0.08)
P32	0.032	0.034	0.035	0.035	0.042	-0.139	-0.061	0.732	0.38	0.50	89.3 (0.02)
P33	0.046	0.046	0.046	0.046	0.049	-0.127	-0.012	0.691	0.28	0.36	88.7 (0.02)
P34	-0.019	-0.019	-0.019	-0.019	-0.029	-0.213	-0.131	0.676	0.43	0.55	86.5 (0.03)
P35	-0.172	-0.172	-0.172	-0.172	-0.139	-0.155	-0.166	0.576	0.38	0.46	85.9 (0.04)

Poor Patient ID	Wavelet Correlations (scale λ_j)								Rudge et al. (2006b) diagnostics		Chase et al. (2004) diagnostics
	λ_1	λ_2	λ_3	λ_4	λ_5	λ_6	λ_7	λ_8	AND	RAND	TI(SE)
Poor Median	**-0.019**	**-0.019**	**-0.019**	**-0.019**	**-0.008**	**-0.139**	**0.040**	**0.676**	**0.390**	**0.500**	**85.2**
(95%CI)	(-0.092, 0.013)	(-0.094, 0.013)	(-0.094, 0.013)	(-094, 0.013)	(-0.069, 0.032)	(-0.195, -0.091)	(-0.147, -0.003)	(0.636, 0.736)	(0.343, 0.515)	(0.444, 0.620)	(81.333, 87.001)
Good Pt ID											
	λ_1	λ_2	λ_3	λ_4	λ_5	λ_6	λ_7	λ_8	AND	RAND	TI(SE)
P1	-0.112	-0.134	-0.134	-0.134	-0.107	-0.101	-0.115	0.662	0.51	0.62	87.0 (0.04)
P3	-0.503	-0.504	-0.504	-0.504	-0.439	-0.221	-0.242	0.675	0.70	0.83	88.8 (0.02)
P5	0.074	0.073	0.073	0.073	0.078	-0.118	-0.004	0.707	0.60	0.80	91.1 (0.02)
P6	-0.202	-0.202	-0.202	-0.202	-0.155	-0.090	-0.167	0.666	0.70	0.84	87.0 (0.01)
P8	0.208	0.206	0.206	0.206	0.211	-0.029	0.081	0.783	0.45	0.59	87.4 (0.03)
P12	-0.359	-0.359	-0.359	-0.359	-0.316	-0.264	-0.179	0.645	0.61	0.77	84.1 (0.03)
P13	0.258	0.258	0.258	0.258	0.257	0.007	0.107	0.768	0.37	0.45	86.1 (0.07)
P14	-0.378	-0.379	-0.380	-0.380	-0.301	-0.074	-0.003	0.785	0.48	0.56	93.1 (0.03)
P15	0.086	0.092	0.093	0.093	0.084	-0.149	-0.039	-0.697	0.45	0.60	91.1 (0.01)
P16	0.168	0.169	0.169	0.169	0.173	-0.067	0.035	0.758	0.44	0.57	87.9 (0.02)
P17	-0.122	-0.122	-0.122	-0.122	-0.069	0.131	-0.161	0.604	0.61	0.72	84.0 (0.04)
P18	-0.134	-0.134	-0.134	-0.134	-0.130	-0.243	-0.211	0.628	0.55	0.68	94.6 (0.03)
P19	0.272	0.273	0.273	0.273	0.277	0.066	0.195	0.726	0.50	0.66	91.1 (0.01)
P20	0.057	0.057	0.057	0.057	0.057	-0.106	-0.051	0.613	0.53	0.65	87.3 (0.03)
P23	0.149	0.149	0.149	0.149	0.164	-0.019	0.099	0.729	0.72	0.85	84.8 (0.11)
P24	0.231	0.232	0.232	0.232	0.232	-0.007	0.157	0.793	0.43	0.54	88.1 (0.02)
P25	-0.211	-0.214	-0.214	-0.214	-0.188	-0.218	-0.185	0.561	0.50	0.66	92.4 (0.03)
P26	-0.122	-0.123	-0.123	-0.123	-0.073	0.057	-0.011	0.579	0.68	0.88	87.4 (0.03)
P30	-0.045	-0.044	-0.044	-0.044	-0.049	-0.208	-0.150	0.647	0.63	0.82	92.2 (0.02)
P31	0.040	0.040	0.040	0.040	0.047	-0.108	0.024	0.701	0.40	0.51	89.3 (0.03)
P36	0.081	0.081	0.081	0.081	0.055	-0.172	-0.104	0.677	0.52	0.64	86.4 (0.10)
P37	0.272	0.273	0.273	0.273	0.273	0.066	0.195	0.726	0.53	0.59	79.9 (0.09)
Good Median	**0.049**	**0.049**	**0.0485**	**0.0485**	**0.051**	**-0.096**	**-0.025**	**0.676**	**0.525**	**0.655**	**87.7**
(95%CI)	(-0.122, 0.149)	(-0.134, 0.149)	(-0.134, 0.149)	(-0.134, 0.149)	(-0.108, 0.164)	(-0.149, -0.019)	(0.015, 0.036)	(0.065, -0.726)	(0.479, 0.610)	(0.590, 0.771)	(86.984, 91.100)
Kruskal Wallis P value (Poor vs Good)	P=0.32	0.32	0.32	0.32	0.30	0.16	0.40	0.84	**0.004**	**0.003**	**0.005**

Table 5. Kruskal Wallis test on the wavelet correlation, and on Rudge et al.'s (2006b) and Chase et al.'s (2004) diagnostics – testing for differences between the DWT based poor versus good tracker groups.

Variable	Poor group median	Good group median	k-w#: P value
Modulus WCORR at λ_1	0.046	0.159	**0.001**
"Count of NS"	**5**	**2**	**0.001**
AND	0.39	0.53	**0.004**
RAND	0.50	0.66	**0.003**
TI	85.20	87.7	**0.005**

Table 6. K-W tests of all wavelet and other diagnostics by wavelet based tracking group.
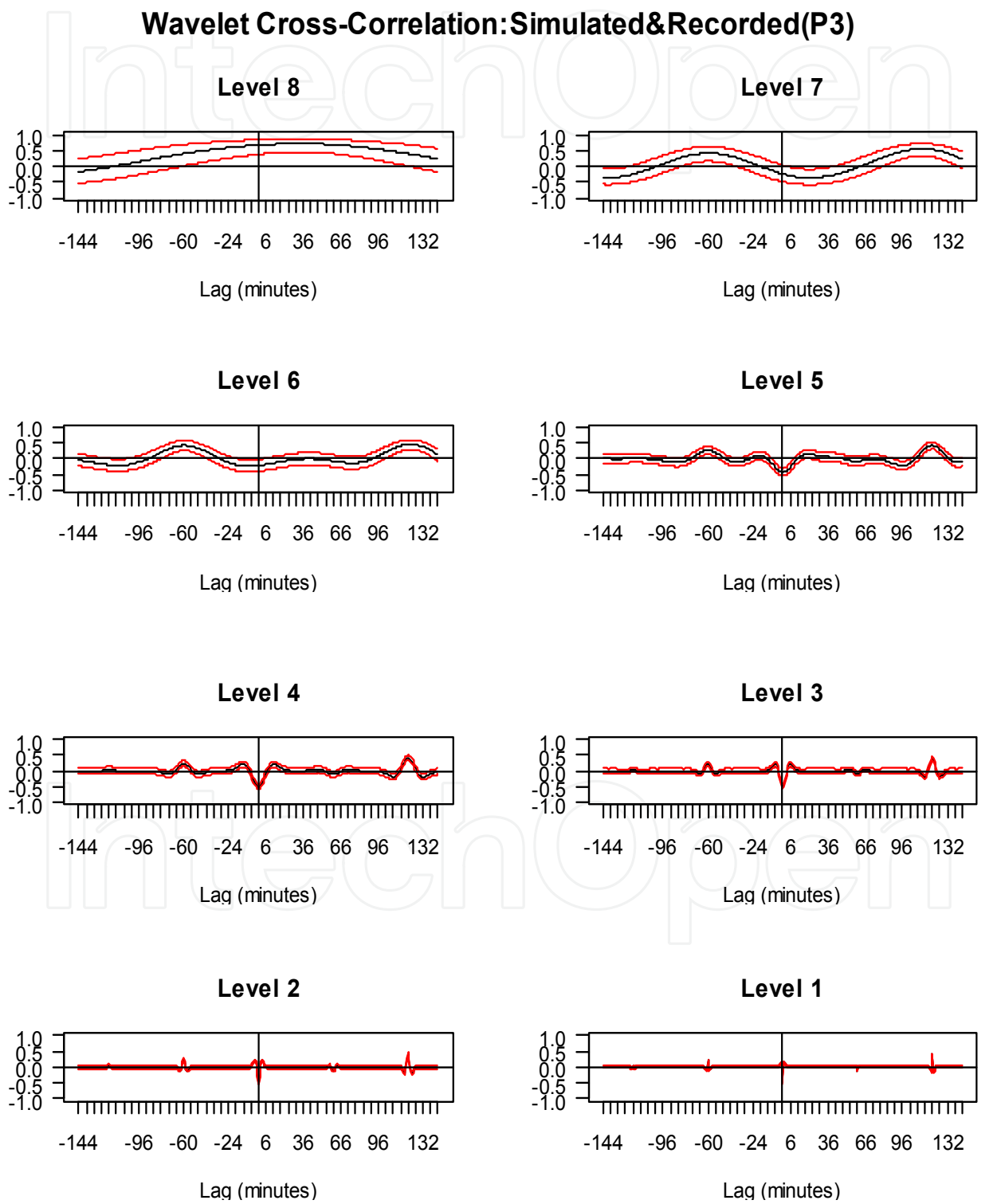
3.3 Using the Wavelet Cross-Correlation (WCCORR)

We can investigate possible lead or lag relationships between a given patient's modelled (simulated) versus observed (recorded) A-S profile by examining a plot of its MODWT based wavelet cross-correlation (WCCORR), according to Equation (8). Figure 8 shows this WCCORR plot for Patient 3 (P3: a good tracker) and Patient 4 (P4: a poor tracker). For Patient 3 the $\tilde{\rho}$ values are negative and statistically significant for all scales except 8 (Table 7), and there is also a large positive peak at a lag of 120 minutes for the first six wavelet scales λ_j (j=1, 2, ..., 6) (Figure 8). At scale λ_7; a large positive peak occurs at 112 minutes for Patient 3; and at scale λ_8 at a lag of 33 minutes. We conclude that at scale λ_7 there is a period of 170 minutes (see Figure 15) for Patient 3. Likewise an examination of Figure 8 shows an inverse shaped profile of peaks to troughs for Patient 4 (a poor tracker), with generally non-significant positive $\tilde{\rho}$ values compared to Patient 3 (see also Table 7). It is noteworthy from Figure 8 that generally patients who are good trackers show a common type of WCCORR signature or pattern, with WCCORR being significant at zero lag (for all scales) and their 95% CI do not include zero (see Table 7), not so for the poor trackers.

Patient 3 (good tracker)								
Scale	Level 1	Level 2	Level 3	Level 4	Level 5	Level 6	Level 7	Level 8
L. CI	-0.528	-0.539	-0.554	-0.573	-0.544	-0.398	-0.485	0.382
$\tilde{\rho}$	-0.503[+]	-0.504[+]	-0.504[+]	-0.504[+]	-0.439[+]	-0.221[+]	-0.242[+]	0.675[+]
U. CI[++]	-0.477	-0.467	-0.451	-0.428	-0.321	-0.027	0.036	0.845

Patient 4 (poor tracker)								
Scale	Level 1	Level 2	Level 3	Level 4	Level 5	Level 6	Level 7	Level 8
L. CI	-0.034	-0.050	-0.074	-0.107	-0.123	-0.297	-0.299	0.401
$\tilde{\rho}$	0.006	0.006	0.005	0.006	0.036	-0.077	0.023	0.724
U. CI[++]	0.045	0.061	0.085	0.117	0.194	0.151	0.339	0.886

Table 7. The signature of WCORR for the Patient 3 and Patient 4 at zero lag based WCCORR. The positive subscript (+) indicates significant WCCORR $\tilde{\rho}$ values.

Recall that Table 7 gives the values (*signature* over wavelet scales) of $\tilde{\rho}$ and their associated 95% confidence limits (L.CI, U.CI) for Patient 3 and Patient 4 who are deemed, to be a good and poor tracker, respectively (as depicted by Figure 8). The main results of the work in this chapter are summarised in Table 8 and discussed in detail in the Conclusion (section 4).
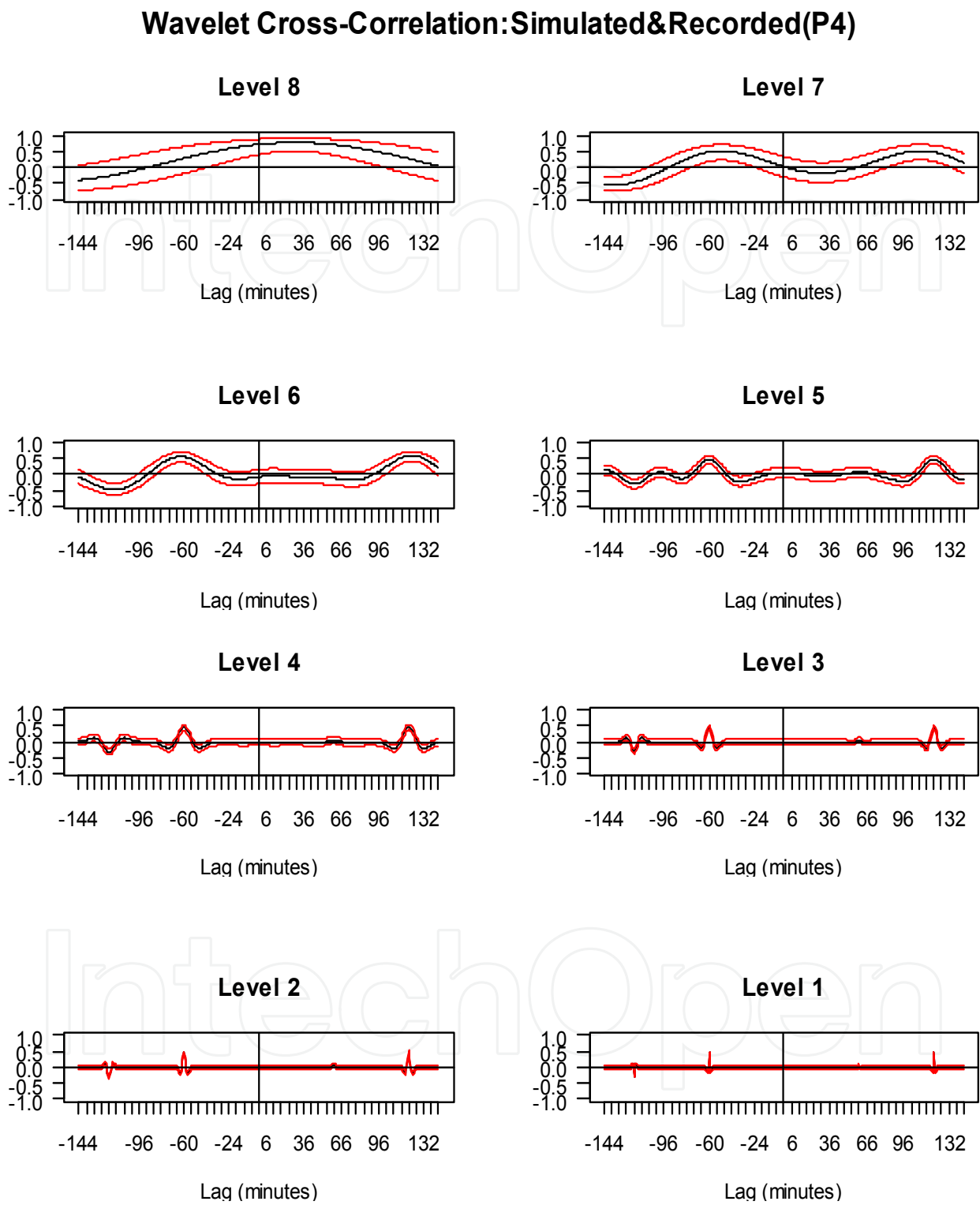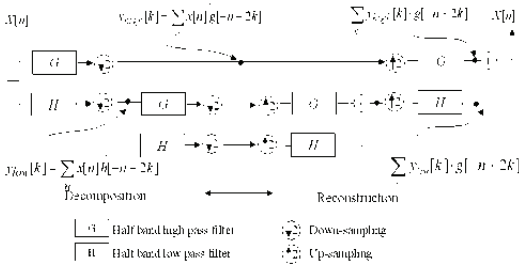
Wavelet Cross-Correlation:Simulated&Recorded(P3)

Wavelet Cross-Correlation:Simulated&Recorded(P4)

Fig. 8. MODWT estimated wavelet Cross-Correlation between the simulated and recorded infusion series for lags up to ±144 minutes for Patient 3 (a good tracker) and Patient 4 (a poor tracker) with approximate 95% CI (red broken lines).

Table 8. Overview of DWT and WCORR results.

Authors	Equations or Model used	Mathematical methods used	Aims of the study and the performan indicators derived
Kang et al. (this chapter)	See the schema of our approach of Chapter 2 below: **DWT Procedure (second stage)** **DWT analysis and synthesis equations** $X = [X_1, X_2,..., X_N]$, $N=2^J$, DWT analysis equation $W = \mathcal{W}X$ W= discrete wavelet coefficients, $\mathcal{W}$= $N \times N$ orthonormal matrix $W = \mathcal{W}X, W = \left[W_1, W_2, \cdots, W_J, V_J \right]^T, \mathcal{W} = \left[\mathcal{W}_1, \mathcal{W}_2, ..., \mathcal{W}_J, \mathcal{V}_J \right]$ $X = \mathcal{W}^T W = \left[\mathcal{W}_1, \mathcal{W}_2, ..., \mathcal{W}_J, \mathcal{V}_J \right]^T \left[W_1, W_2, ..., W_J, V_J \right]^T$ $= \sum_{j=1}^{J} \mathcal{W}_j^T W_j + \mathcal{V}_J^T V_J \quad \Rightarrow$ DWT synthesis equation **DWT − MRA** $X = \sum_{j=1}^{J} \mathcal{W}_j^T W_j + \mathcal{V}_J^T V_J = \sum_{j=1}^{J} D_j + S_J \Rightarrow$ Additive decomposition(=MRA) $D_j = \mathcal{W}_j^T W_j$: Portion of synthesis due to scale λ_j, jth 'detail' $S_J = \mathcal{V}_J^T V$: 'smooth' of Jth order	Discrete Wavelet Transform (DWT) (Percival & Walden, 2000) Maximal Overlap Discrete Wavelet (MODWT) (Percival & Walden, 2000) Multiresolution analysis (MRA) (Percival & Walden, 2000) DWT-MRA, MODWT-MRA	Develop a wavelet correlation (WC and wavelet cross-correlation (WC approach for assessing the validity deterministic dynamic models agai empirical agitation-sedation data of patients. Provide graphical assessment tool wavelet based numerical metri comparability between the model a data via the discrete wavelet tran (DWT), partial DWT (PDWT), m overlap DWT (MODWT) and Multiresolution analysis (MRA). Investigate the lag/lead relatio between the simulated and re infusion series on a scale by scale ba wavelet cross-correlation (WC methods. Develop performance measures as fo 1. Modulus of the w correlation at wavelet s λ_1. 2. Count number (out of the number of non-sign wavelet correlations at λ_j (j=1,2,…,8). Test poor versus good fit or tracking groups via the: Kruskal Wallis test on the W measures per patient and on the ind in 1 and 2 above to test for differences (for the poor versus trackers group).

4. Conclusion

DWT and MODWT-MRA decomposition and reconstruction are shown to provide clear and consistent, in regard to good or poor performance, "signatures" of, and values for the wavelet correlations and cross-correlations (at all dyadic scales) between an ICU patient's bivariate time series, namely their simulated and their recorded A-S infusion profiles over time under sedation. A suite of wavelet techniques are advocated, based on the DWT, and applied successfully to assess whether an ICU patient's mathematically simulated agitation-sedation (A-S) status reflects their true dynamic profile.

The wavelet correlation profiles of the good trackers are shown to be invariably significant at all scales (except at 32 and 64). Patients who exhibit poor tracking exhibit WCORR profiles which are invariably non significant at almost all wavelet scales, *particularly* at λ_1. Moreover, *cross*-correlation (WCCORR) signatures also show a common pattern for the good trackers, which is distinctly different to the pattern associated with poor tracking. It is also shown that the lead or lag relationship between a patient's simulated and recorded agitation-sedation infusion series can be investigated on a scale by scale basis via the implementation of the MODWT-MRA. The MRA is shown to successfully indicate local features of interest in the simulated and recorded series, with the smooth MRA series offering a good visual summary of the overall long-term trends in a patient's A-S status.

Fifteen poor trackers are identified by the DWT based diagnostics derived in this chapter. Specifically it is found that the modulus of WCORR at λ_1, $|\lambda_1|$, is invariably higher (and significantly so) for the good compared to the poor trackers. The profile of ("Count of NS") across all patients is higher for the poor trackers; and the values of RAND, AND and $|\lambda_j|$ invariably higher for the good trackers. Specifically the median absolute value of the wavelet correlation at λ_1, and median value of AND, RAND and TI are highly significantly lower for the poor trackers (15 of 37 patients). The median of the number of non significant wavelet correlations (the "Count of NS" variable) is 5.0 for the poor trackers, significantly higher than the median of 2.0 for the good tracking group (P = 0.001). It is noteworthy that 11 of the 15 DWT based poor trackers are also found to be poor trackers by either or both of Rudge et al.'s (2006b) and Chase et al.'s (2004) (non wavelet based) performance indicators, showing significant agreement between the wavelet DWT and the earlier kernel based methods - with a kappa test of agreement between the WCORR criterion for poor tracking and Chase et al (2004) of 0.2127 (P=0.01); and with Rudge et al. (2006b) of 0.5856 (P=0.001).

Other recent work by Kang et al. (*In Prep)* has used Bayesian densities and wavelet shrinkage methods to create a novel wavelet probability band (WPB). A 90% value for the WPB implies that for at least 90% of the time, the estimated mean value of the patient's recorded infusion rate lies within the band. A 90% WPB was constructed by Kang et al. *(In Prep*) for each of the 37 patient profiles, and the time and duration of any deviations from the wavelet probability band recorded for each patient. Likewise wavelet analogues of the AND and RAND diagnostics of Rudge et al. (2006a; 2006b), namely the average normalized wavelet density (ANWD) and the relative average normalized wavelet density (RANWD) have been derived by Kang et al. *(In Prep)*; as has a Wavelet Time Coverage Index (WTCI) – all by using Bayesian wavelet thresholding. The resultant WTCI and 90% WPB provide very strong support for the DWT wavelet diagnostics derived in this chapter. Indeed of the 15 DWT based poor trackers identified in this chapter, 10 also

exhibit a low WPB (WPB 90% < 70%) and a low wavelet density based RANWD measure (RANWD ≤ 0.5) and are likewise deemed to be poor trackers according to these recent wavelet regression methods of Kang et al. (*In Prep*). Statistically speaking the wavelet probability band and wavelet density diagnostics mirror the poor versus good classification of this chapter's WCORR DWT based diagnostics (kappa = 0.7701, P = 0.0001). The main reason for the reduced total time within the WPB (and for the non significant WCORRs) for this minority group of 10 (or 15) poor trackers (of a total of 37 patients), is the consistently poor performance of the DE model throughout their *total* length of the A-S simulation.

The work in this chapter provides a suite of new wavelet based diagnostics by which to achieve statistical model validation of the A-S models. The DWT, wavelet correlation and cross-correlation measures derived in this chapter are proved to be valid for assessing control, and mirror earlier validation measures; as do the more recent wavelet regression diagnostics (namely WTCI, ANWD, RANWD, and WPB 90%) of Kang et al. (*In Prep*). Wavelets are shown to visually and quantitatively discriminate patients for whom the A-S model captures their fundamental A-S dynamics, versus those, for whom this is not so. Wavelet WCORR and WCCORR signatures thus form a possibly alternative and appropriate feedback mechanism for comparison of improved sedation administration controllers and gain. The wavelets based visual tools and quantitative measures thus contribute to the task of improving and of refining A-S models. This chapter thus demonstrates that wavelets provide a new diagnostic tool by which to assess the agitation-sedation of ICU patients, and show that it is possible to evaluate A-S models via wavelet diagnostics for accurate evaluation of A-S management, where the latter represents a trade-off between the benefits of low patient agitation versus the cost of high infusion rates and increased total dose requirements (Rudge et al., 2003; 2005; 2006a; 2006b). Wavelets are thus suitable for clinical implementation in ICU agitation and sedation control.

Overall the various wavelet diagnostics strongly agree and confirm the value of A-S modelling in ICU. Wavelet DWT analysis also demonstrates that the models of the A-S studies of Chase et al., (2004), Rudge et al., (2005; 2006a; 2000b) and of Lee et al., (2005), are suitable for developing more advanced optimal infusion controllers. These offer significant clinical potential of improved agitation management and reduced length of stay in critical care. The use of quantitative modelling to enhance understanding of the A-S system and the provision of an A-S simulation platform are critical tools in this area of patient critical care.

The DWT approach gives robust performance metrics of A-S control and also yields excellent visual assessment tools - generalisable to any study which investigates the similarity or closeness between any bivariate time series of, say, a large number of units (patients, households etc) and of disparate lengths and possibly of extremely long length.

5. References

Abramovich, F., & Benjamini, Y. (1995). Thresholding of wavelet coefficients as multiple hypotheses testing procedure. *Lecture Notes in Statistics, 103*, 5-14.

Allan, D. W. (1966). Statistics of atomic frequency standards. *Proceedings of the IEEE, 54*(2), 221-230.

Barber, S., Nason, G. P., & Silverman, B. W. (2002). Posterior probability intervals for wavelet thresholding. *Journal of the Royal Statistical Society. Series B (Statistical Methodology), 64*(2), 189-205.

Chang, S. G., Yu, B., & Vetterli, M. (2000a). Spatially adaptive wavelet thresholding based on context modeling for image denoising. *IEEE Transactions on Image Processing, 9*(9), 1522- 1531.

Chang, S. G., Yu, B., & Vetterli, M. (2000b). Adaptive wavelet thresholding for image denoising and compression. *IEEE Transactions on Image Processing, 9*(9), 1532-1546.

Chase, J. G., Rudge, A. D., Shaw, G. M., Wake, G. C., Lee, D., Hudson, I. L., et al. (2004). Modeling and control of the agitation-sedation cycle for critical care patients. *Medical Engineering and Physics, 26*(6), 459-471.

Chui, C. K. (1992). *An introduction to wavelets*: Academic Press.

Daubechies, I. (1992). *Ten lectures on wavelets*. Philadelphia: Society for Industrial and Applied Mathematics.

Donoho, D. L. (1995). De-noising by soft-thresholding. *IEEE Transactions on Information Theory, 41*(3), 613-627.

Donoho, D. L., & Johnstone, I. M. (1994). Ideal spatial adaptation via wavelet shrinkage. *Biometrika, 81*, 425-455.

Dépué M (2003). Continuous variables. In: Jolliffe IT, Stephenson DB (eds) Forecast verification: a practitioner's guide in atmospheric science. John Wiley and Sons, Chichester, pp 97–120

Dose V, Menzel A (2004). Bayesian analysis of climate change impacts in phenology. Glob Fraser, G. L., & Riker, R. R. (2001b). Monitoring sedation, agitation, analgesia, and delirium in critically ill adult patients. *Crit Care Clin, 17*(4), 967-987.

Gencay, R., Selcuk, F., & Whitcher, B. (2001). *An introduction to wavelets and other filtering methods in finance and economics*: Academic Press.

Goupillaud, P., Grossmann, A., & Morlet, J. (1984). Cycle-octave and related transforms in seismic signal analysis. *Geoexploration, 23*(1), 85-102.

Haar, A. (1910). Zur Theorie der orthogonalen Funktionensysteme. *Mathematische Annalen, 69*(3), 331-371.

Hudson, I.L. (2011). Meta analysis, in *Encyclopedia of Climate and Weather*, S. H. Schneider, M. Mastrandrea and T. L. Root, (eds), pp 273-287, Oxford University Press.

Hudson, I.L. (2010). Interdisciplinary approaches: towards new statistical methods for phenological studies, *Climatic Change*, 100(1), 143-171.

Hudson, I. L., Keatley, M. R., & Roberts, A. M. I. (2005). Statistical Methods in Phenological Research. Proceedings of the Statistical Solutions to Modern Problems. Proceedings of the 20th International Workshop on Statistical Modelling, eds. AR Francis, KM Matawie, A Oshlack & GK Smyth, ISBN 1 74108 101 7, Sydney, Australia, 10-15 July 2005, pp. 259-270.

Hudson, I.L., & Keatley, M. R. (2010). *Phenological Research: Methods for Environmental and Climate Change Analysis*: Springer, Dordrecht, Netherlands.

Hudson, I.L., Kang, I., & Keatley, M. R. (2010a). Wavelet Analysis of Flowering and Climatic Niche Identification. In I. L. Hudson & M. R. Keatley (Eds.), *Phenological Research: Methods for Environmental and Climate Change Analysis*, pp 361-391, Springer, Dordrecht, Netherlands.

Hudson, I.L., Keatley, M. R., & Kang, I. (2010b). Wavelet characterisation of eucalypt flowering and the influence of climate. *Environmental and Ecological Statistics.* (Doi 10.1007/s10651-010-0149-5).

Hudson I.L., Keatley, M.R., & Kang, I. (2011a) Wavelets and clustering: methods to assess synchronization. pp. 59-70. In: del Valle M, Muñoz R, Gutiérrez JM (eds) *Wavelets: Classification, Theory and Applications*. Nova Science Publishers.

Hudson, I.L., Keatley, M.R., & Kang, I. (2011b). Wavelet Signatures of Climate and Flowering: Identification of Species Groupings In: Olkkonen H (ed) *Discrete Wavelet Transforms / Book 2*. InTech, Vienna, Austria, http://www.intechweb.org ISBN 979-953-307-241-7. (pp 00-30) *(in Press)*

Jaarsma, A. S., Knoester, H., van Rooyen, F., & Bos, A. P. (2001). Biphasic positive airway pressure ventilation (pev+) in children. *Crit Care Clin, 5*(3), 174-177.

Kang, I., Hudson, I. L., & Keatley, M. R. (2004). *Wavelet analysis in phenological research-the study of four flowering eucalypt species in relation to climate.* Paper presented at the International Biometrics Conference (IBC 04), July, Cairns, Australia.

Kang, I., Hudson, I. L., Rudge, A. D., & Chase, J. G. (2005). *Wavelet signature of Agitation-Sedation profiles of ICU patients.* In: Francis AR, Matawie KM, Oshlack A, Smyth GK (eds) Statistical Solutions to Modern Problems. 20th International Workshop on Statistical Modelling, Sydney, July 10–15, University of Western Sydney (Penrith), pp 293-296, ISBN 1 74108 101 7.

Kang, I., Hudson, I. L, Rudge, A, Chase, G. Density estimation and wavelet thresholding via Bayesian methods: application to ICU data, *Computer Methods and Programs in Biomedicine (In prep).*

Kress, J. P., Pohlman, A. S., & Hall, J. B. (2002). Sedation and analgesia in the intensive care unit. *Am J Respir Crit Care Med, 166*(8), 1024-1028.

Kumar, P. (1994). Role of coherent structures in the stochastic-dynamic variability of precipitation. *Journal of Geophysical Research-Atmospheres, 101(D21)*(26), 393-404.

Kumar, P., & Foufoula-Georgiou, E. (1993). A multicomponent decomposition of spatial rainfall fields. 1. Segregation of large- and small-scale features using wavelet transforms. *Water Resources Research, 29*(8), 2515-2532.

Lee, D. S., Rudge, A. D., Chase, J. G., & Shaw, G. M. (2005). A new model validation tool using kernel regression and density estimation. *Computer Methods and Programs in Biomedicine, 80*, 75-87.

Mallat, S. (1989). A theory for multiresolution signal decomposition: the wavelet representation. *IEEE Transactions on Pattern analysis and Machine Intelligence, 11*, 674-693.

McCoy, E. J., Percival, D. B., & Walden, A. T. (1995). *Spectrum estimation via wavelet thresholding of multitaper estimators*. Imperial College, London.

Meyer, F. G. (2003). Wavelet-based estimation of a semiparametric generalized linear model of fMRI time-series. *IEEE Transactions on Medical Imaging, 22*(3), 315-322.

Minto, C. F., Schnider, T. W., Short, T. G., Gregg, K. M., Gentilini, A., & Shafer, S. L. (2000). Response surface model for anesthetic drug interactions. *Anesthesiology, 92*(6), 1603-1616.

Morlet, J. (1983). Sampling theory and wave propagation. *Issues in Acoustic Signal/Image Processing and Recognition, 1*, 233-261.

Ogden, R. T. (1997). *Essential Wavelets for Statistical Applications and Data Analysis*. Boston: Birkhäuser.

Percival, D. B., & Guttorp, P. (1994). Long-memory processes, the Allan variance and wavelets, in *Wavelets and Geophysics*, edited by E. Foufoula-Georgiou and P. Kumar, Vol. 4, *Wavelet Analysis and Its Applications*, 325–344, Academic Press, San Diego, California.

Percival, D. B., & Mofjeld, H. O. (1997). Analysis of subtidal coastal sea level fluctuations using wavelets. *Journal of the American Statistical Association, 92*(439), 868-880.

Percival, D. B., & Walden, A. T. (2000). *Wavelet Methods for Time Series Analysis*. Cambridge, England: Cambridge University Press.

Ramsay, M. A., Savege, T. M., Simpson, B. R., & Goodwin, R. (1974). Controlled sedation with alphaxalone-alphadolone. *Br Med J, 2*(920), 656-659.

Riker, R. R., Picard, J. T., & Fraser, G. L. (1999). Prospective evaluation of the Sedation-Agitation Scale for adult critically ill patients. *Critical care medicine, 27*(7), 1325-1329.

Rudge, A. D., Chase, J. G., Shaw, G. M., & Lee, D. (2006a). Physiological modelling of agitation-sedation dynamics including endogenous agitation reduction. *Medical Engineering & Physics, 28*(7), 629-638.

Rudge, A. D., Chase, J. G., Shaw, G. M., & Lee, D. (2006b). Physiological modelling of agitation-sedation dynamics. *Medical Engineering and Physics, 28*(1), 49-59.

Rudge, A. D., Chase, J. G., Shaw, G. M., Lee, D., Wake, G. C., Hudson, I. L., et al. (2005). Impact of control on agitation-sedation dynamics. *Control Engineering Practice, 13*(9), 1139-1149.

Sessler, C. N., Gosnell, M. S., Grap, M. J., Brophy, G. M., O'neal, P. V., Keane, K. A., et al. (2002). The Richmond agitation-sedation scale: validity and reliability in adult intensive care unit patients. *Am J Respir Crit Care Med, 166*(10), 1338-1344.

Swelden, W. (1996). Wavelets: what next? *Proceedings of the IEEE, 84*(4), 680-685.

Vidakovic, B. (1999). *Statistical modelling by wavelets*. New York: John Wiley & Sons.

Wand, M. P., & Jones, M. C. (1995). *Kernel smoothing*: Chapman & Hall/CRC.

Whitcher, B., Guttorp, P., & Percival, D. B. (2000). Wavelet Analysis of Covariance with Application to Atmospheric Time Series. *Journal of Geophysical Research, 105*(D11), 14,941-962.

Discrete Wavelet Transforms - Biomedical Applications

Edited by Prof. Hannu Olkkonen

ISBN 978-953-307-654-6

Hard cover, 366 pages

Publisher InTech

Published online 12, September, 2011

Published in print edition September, 2011

The discrete wavelet transform (DWT) algorithms have a firm position in processing of signals in several areas of research and industry. As DWT provides both octave-scale frequency and spatial timing of the analyzed signal, it is constantly used to solve and treat more and more advanced problems. The present book: Discrete Wavelet Transforms - Biomedical Applications reviews the recent progress in discrete wavelet transform algorithms and applications. The book reviews the recent progress in DWT algorithms for biomedical applications. The book covers a wide range of architectures (e.g. lifting, shift invariance, multi-scale analysis) for constructing DWTs. The book chapters are organized into four major parts. Part I describes the progress in implementations of the DWT algorithms in biomedical signal analysis. Applications include compression and filtering of biomedical signals, DWT based selection of salient EEG frequency band, shift invariant DWTs for multiscale analysis and DWT assisted heart sound analysis. Part II addresses speech analysis, modeling and understanding of speech and speaker recognition. Part III focuses biosensor applications such as calibration of enzymatic sensors, multiscale analysis of wireless capsule endoscopy recordings, DWT assisted electronic nose analysis and optical fibre sensor analyses. Finally, Part IV describes DWT algorithms for tools in identification and diagnostics: identification based on hand geometry, identification of species groupings, object detection and tracking, DWT signatures and diagnostics for assessment of ICU agitation-sedation controllers and DWT based diagnostics of power transformers.The chapters of the present book consist of both tutorial and highly advanced material. Therefore, the book is intended to be a reference text for graduate students and researchers to obtain state-of-the-art knowledge on specific applications.

How to reference

In order to correctly reference this scholarly work, feel free to copy and paste the following:

INTECH
open science | open minds

Slavka Krautzeka 83/A
51000 Rijeka, Croatia
Phone: +385 (51) 770 447
Fax: +385 (51) 686 166
www.intechopen.com

No.65, Yan An Road (West), Shanghai, 200040, China
中国上海市延安西路65号上海国际贵都大饭店办公楼405单元
Phone: +86-21-62489820
Fax: +86-21-62489821